

## ABSTRACT

Title: TERRESTRIAL ALTERATION OF CM2  
CHONDRITIC CARBONATES IN A SUITE  
OF PAIRED ANTARCTIC METEORITES..

Mark Anthony Tyra, MSc, 2005

Directed By: Assistant Professor, James Farquhar, Department  
of Geology

The  $\delta^{18}\text{O}$ ,  $\delta^{17}\text{O}$ ,  $\delta^{13}\text{C}$ , and  $\delta^{14}\text{C}$  compositions of carbonate grains were measured from paired Antarctic CM2 chondrites (EET96006, EET96016, EET96017, and EET96019). Oxygen isotopic compositions reveal both terrestrial and extraterrestrial carbonate sources. Bulk  $\delta^{13}\text{C}$  and  $\delta^{14}\text{C}$  measurements suggest at least two terrestrial carbonate components: 1) carbonate derived from equilibration of atmospheric  $\text{CO}_2$  with silicates during weathering reactions, and 2) carbonate derived from a second undefined source. Oxygen and carbon isotope data suggest that silicate weathering reactions drove oxygen isotopic composition of Antarctic water away from the terrestrial fractionation line (TFL) ( $\Delta^{17}\text{O} \leq 3.6\text{‰}$ ). Further oxygen isotopic compositional constraints were placed by Secondary Ionization Mass Spectrometry (SIMS) of *in-situ* carbonates. We suggest three sources for meteoritic carbonate: 1) primary calcite formed in the presence of evolving planetesimal water and 2) secondary calcite derived from alkalinity laden terrestrial water and 3) alkalinity formed as the result of weathering of meteoritic silicates.



TERRESTRIAL ALTERATION OF CM2 CHONDRITIC CARBONATES IN A  
SUITE OF PAIRED ANTARCTIC METEORITES.

By

Mark Anthony Tyra

Thesis submitted to the Faculty of the Graduate School of the  
University of Maryland, College Park, in partial fulfillment  
of the requirements for the degree of  
Master of Science  
2005

Advisory Committee:  
Assistant Professor James Farquhar, Chair  
Professor Richard J. Walker  
Associate Professor Alan J. Kaufman

© Copyright by  
Mark Anthony Tyra  
2005

## Preface

This dissertation is presented in four sections. Chapter 1 gives an overview of the project. Chapter 2 is preparation for submittal to *Geochimica et Cosmochimica Acta*, and chapter 3 contains supplemental data and interpretations that augment chapter 2. With the collection of additional data chapter 3 will also be submitted for publication. Chapter 4 offers conclusions. Page numbers, tables, and figures are in sequence. Although the two manuscripts (chapters 2 and 3) will be submitted as multi-author documents, they were written by the lead author and represent this original contribution.

## Foreword

Our species needs, and deserves, a citizenry with minds wide awake and a basic understanding of how the world works.

Carl Sagan

## **Dedication**

This work is dedicated to my family, for without their support, I would never be who I am today. From my dad, my curiosity. From my mom, my creativity and ability to doodle and doodle well (which really helps sometimes). And from my brother, aunts, uncles, cousins, and grandparents, a feeling of stability and love. Most especially, I thank my wife, Jennifer, for putting up with my flights of fancy and jaunts all over the country. I also owe her thanks for her guiding hand as she asks me “Why are you thinking about font and references when you haven’t even finished the paper?” It is our priorities that matter, and I thank her for her love, humor, and support.

## Acknowledgements

So many have helped along the way... I would like to thank James Farquhar for being not only my advisor, but someone who always puts things in a way I never would have thought. Learning to look at the ordinary in a different light is one of his gifts. I also thank my committee members, Jay Kaufman and Richard Walker, for their comments, suggestions, and patience. I also thank Boz Wing, Phil Piccoli, Richard Ash, Gretchen Benedix, Tim Jull, Yunbin Guan, Terry Jackson, Laurie Leshin, Bill McDonough, Tim McCoy, and Ruth Blake for their input into this work. I also thank Sean Timpa, Tom Ireland, Lisa Farquhar, John Jamieson, Margaret Baker, Tracey Centorbi, and Jackie Mann who contributed their time, ideas, and red pen to help this project.

# Table of Contents

Preface.....	ii
Foreword.....	iii
Acknowledgements.....	v
List of Tables .....	vii
Chapter 1: Introduction.....	1
Chapter 2: Terrestrial Alteration of a suite of Antarctic CM2 chondrite meteorites ....	8
2.1 Introduction.....	9
2.2 Analytical Procedures.....	13
2.2.1 Electron Microscopy.....	13
2.2.2 Isotopic Analysis.....	15
2.2.3 Treatment of Isotopic Data .....	20
2.3. Samples.....	20
2.4 Results.....	22
2.4.1 Petrography.....	22
2.4.2 Carbon and Oxygen Isotopic Data.....	24
2.5 Discussion.....	36
2.5.1 Pairing.....	36
2.5.2 Carbonate Formation, Extraterrestrial and Terrestrial.....	36
2.5.2.1 Evidence from Oxygen Isotopes.....	41
2.5.2.2 Evidence from Carbon Isotopes.....	43
2.6 Conclusions.....	49
Chapter 3. Oxygen Isotope Heterogeneity in Calcite from CM2 Chondrites.....	52
3.1 Introduction.....	53
3.2 Methods.....	54
3.2.1 Samples.....	54
3.2.2 SEM work .....	54
3.2.3 SIMS .....	55
3.3 Results.....	57
3.4 Discussion.....	59
3.4.1 Comparison of SIMS results with bulk-carbonate data.....	59
3.4.2 Observations and Model .....	62
3.5 Conclusions.....	69
Chapter 4. Work Summary .....	70
Appendix 1.....	73
Appendix 2.....	75
Bibliography .....	80

## List of Tables

<u>Table</u>		<u>Page</u>
Table 1.	Composition of Carbonates within EET96006	14
Table 2.	Description of EET-paired meteorites	21
Table 3.	Various hydrated carbonates sorted by water content	29
Table 4.	C and O isotopic evaluation of paired Elephant Moraine CM2 meteorites	46
Table 5.	Oxygen isotopic compositions within select EET carbonate grains	58

## List of Figures

<u>Figure</u>		<u>Page</u>
Figure 1.	Location of Elephant Moraine in context to other nearby landmarks.	3
Figure 2.	Photograph of Elephant Moraine.	5
Figure 3.	Oxygen isotope signatures of carbonaceous chondrites by type.	10
Figure 4.	Photographs of intact EET96006 and EET96029.	21
Figure 5.	Examples of carbonate found within the EET paired suite	25
Figure 6.	Oxygen isotopic comparison between EET bulk carbonate and CM2 fall bulk carbonate.	30
Figure 7.	The fraction of modern $^{14}\text{C}$ (FMOD $^{14}\text{C}$ ) vs. $\Delta^{17}\text{O}$ in EET finds.	33
Figure 8.	Plot of $\delta^{13}\text{C}$ vs. FMOD $^{14}\text{C}$ and $\Delta^{17}\text{O}$ .	34
Figure 9.	Comparison of CM2 fall carbonates with those found in this study's EET paired set.	38
Figure 10.	Photograph of SIMS at the Arizona State University GEOSIMS laboratory	56
Figure 11.	Three isotope plot ( $\delta^{17}\text{O}$ vs. $\delta^{18}\text{O}$ ) relative to Standard Mean Ocean Water (SMOW) of in-situ matrix carbonates	60
Figure 12.	$\Delta^{17}\text{O}$ vs. $\delta^{18}\text{O}$ for carbonates from this study and bulk carbonate data from Chapter 2	61
Figure 13.	$\Delta^{17}\text{O}$ vs. $\delta^{18}\text{O}$ for <i>in-situ</i> carbonates and CM2 falls	64
Figure 14.	Illustration of a model of carbonate evolution within EET meteorites	67
Figure 15.	Spot locations of EPMA WDS elemental analyses	73
Figure 16.	Spot locations of SIMS oxygen isotopic analyses	75

## **Chapter 1: Introduction**

Meteorites that formed in the vacuum of space are in chemical disequilibrium with conditions on Earth's surface and quickly deteriorate (BUDDHUE, 1957; CASSIDY *et al.*, 1992). Notably, in dry environments chemical weathering is limited and meteorites survive longer than in temperate areas. For this reason, Antarctica has become one of the most productive settings for meteorite collection; because ice flow results in the burial, preservation, and concentration of meteorites on stranding surfaces. For example, the East Antarctic ice sheet flows from kilometer-high domes in all directions, and when this ice abuts the Transantarctic Mountains, summer heating and strong dry winds ablate the ice exposing an abundance of meteorites.

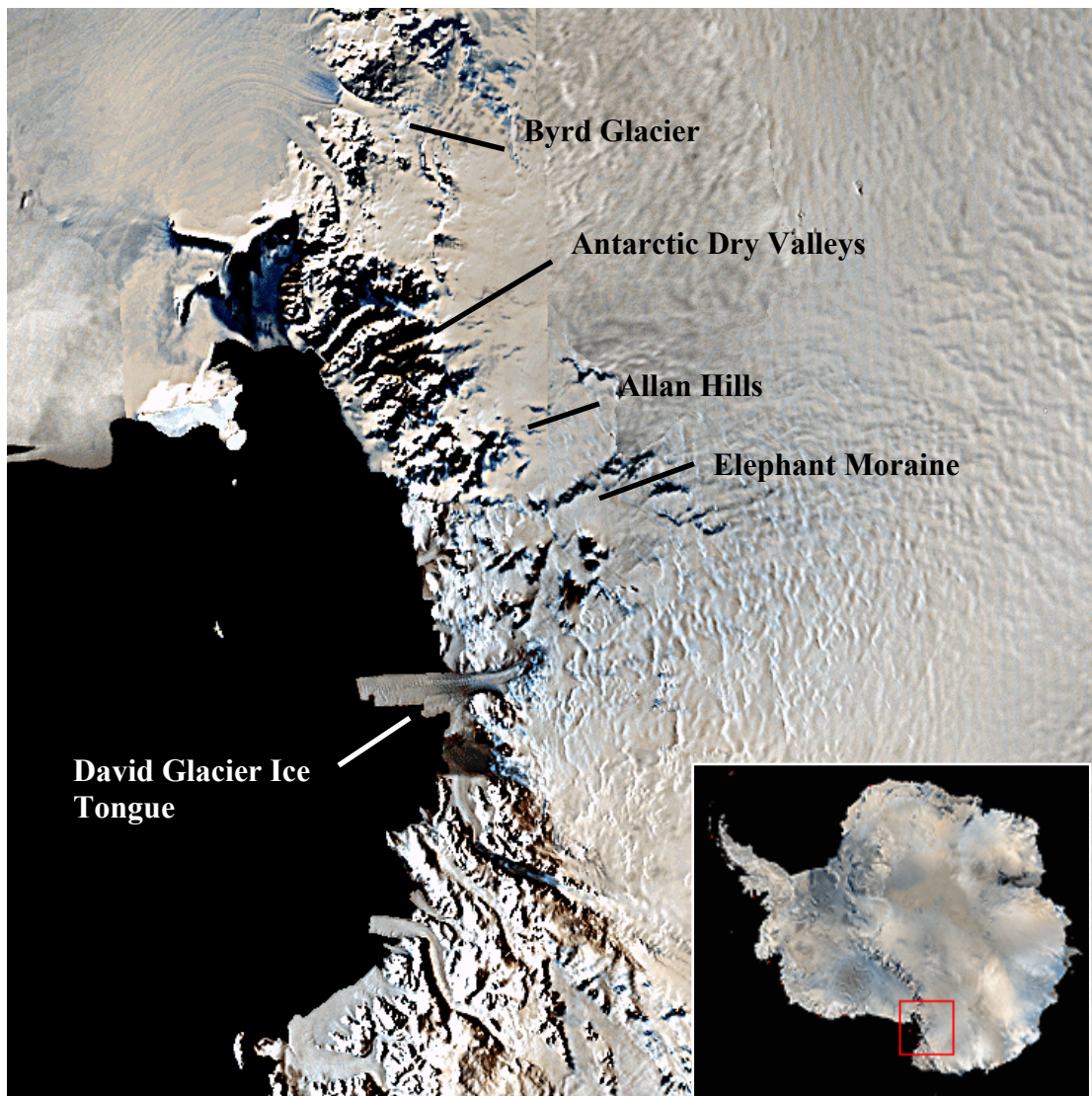
Not only does ice flow meteorite concentration aid researchers in acquiring meteorites, but meteorites also provide information about ice movement which affects them. Meteorites and other lithic clasts found on stranding surfaces have been used to study ice mechanics and flow characteristics (CASSIDY *et al.*, 1992; FAURE, 1990; FAURE and TAYLOR, 1985; HUSS, 1990). One parameter, meteorite terrestrial residence time, has been determined using radionuclide species such as  $^{14}\text{C}$  and  $^{36}\text{Cl}$  located within meteorites which are produced by cosmic-ray spallation reactions (JULL *et al.*, 1989; NISHIZUMI *et al.*, 1989), and natural thermoluminescence (TL) decay (BENOIT, 1995; BENOIT *et al.*, 1994; BENOIT and SEARS, 1992).

In this study we examine paired meteorites from Elephant Moraine, Antarctica (Fig. 1). Paired meteorites are thought to originate from the same parent meteorite that broke up either due to catastrophic atmospheric deceleration or direct impact. Pairings are based upon the proximity of pieces in relation to one another, petrography (including SEM analysis), and other comparisons between pieces. The

**Figure 1.** Location of Elephant Moraine in context to other nearby landmarks.

Images courtesy of United States Geological Survey (USGS) Terraweb

(<http://terraweb.wr.usgs.gov>).



meteorites studied here are CM2 meteorites, a subset of stony meteorites that are among the most ancient solar system material known (See Brearley and Jones (1998) and Kerridge and Matthews (1988) for summaries). Their formation age has been calculated as 4.55 Ga by U/Pb, Rb/Sr, and Sm/Nd isotopic dating techniques (BREARLEY and JONES, 1998).

Spectroscopic observations of CM2 carbonaceous chondrites and asteroids place CM2 meteorite probable parent bodies as being G-class asteroids including 19 Fortuna, 106 Dione, and 13 Egeria (BURBINE, 1998; RIVKIN et al., 2003). These meteorites are characterized by the presence clusters of olivine and pyroxene known as chondrules and small amounts of organic matter. Variable amounts of other phases such as calcite, phosphates, gypsum, whewellite ( $\text{CaC}_2\text{O}_4 \cdot (\text{H}_2\text{O})$ ), and tochilinite ( $(\text{FeS}) \cdot (\text{Mg,Fe})(\text{OH})_2$ ) are also present and are attributed to parent-body aqueous alteration (BREARLEY and JONES, 1998; FUCHS *et al.*, 1973). The CM2 chondrites vary in degree of aqueous alteration, and most have been classified as alteration type 2 (in a 1-3 scale where “3” meteorites have little aqueous alteration and “1” meteorites are so altered no anhydrous minerals remain) (ZOLENSKY et al., 1997). Another mineralogic alteration index has been proposed by Browning *et al.* (1996) that tracks changes to Fe/Si that are attributed to serpentinization of cronstedtite ( $\text{Fe}^{2+}_2\text{Fe}^{3+}_2\text{SiO}_5(\text{OH})_4$ ).

Elephant Moraine (Fig. 2) lies 80 km northwest of the Allan Hills meteorite stranding surface (CASSIDY *et al.*, 1983). While other stranding surfaces are often marked by mountains protruding above the glacial surface physically blocking ice

**Figure 2.** Photograph of Elephant Moraine. Courtesy of David Schutt, Antarctic Meteorite Location and Mapping Project (AMLAMP).



flow, Elephant Moraine consists of a submerged mesa or ridge that is unbroken for at least 90 km (CASSIDY *et al.*, 1992). The moraine forms as the result of upwelling, stagnation, and subsequent ablation of ice due to the physical barrier. However, because the barrier at Elephant Moraine is submerged, the stranding surface may be unstable as an ice-level rise could resume horizontal ice flow (FAURE and TAYLOR, 1985).

Faure and Taylor (1985) determined that Elephant Moraine formed some  $30 \pm 6.5$  Ka ago using ablation rates calculated from direct measurement and assuming constant ice levels. Meteorites in the glacial deposits generally have relatively younger terrestrial ages than at other stranding sites (BENOIT *et al.*, 1994). Terrestrial ages of Elephant moraine meteorites (often designated “EET”) are generally between 35 and 200 ka, and surface exposure TL age is  $<12.5$  ka (BENOIT *et al.*, 1994; NISHIIZUMI *et al.*, 1989). Benoit *et al.* (1994) further suggested that EET meteorites are locally derived insofar as ice flow models suggest deeply buried meteorites do not surface at this location.

Because meteorites from Antarctic stranding surfaces are so important to the meteorite catalogue, finding out how they are altered in the terrestrial environment is of fundamental concern. Antarctic meteorites are often assumed to be preserved within the ice with a minimal degree of chemical alteration. The reality, however, is that once meteorites surface they are subject to many processes that can disturb their chemical distribution and mineral compositions. While it is likely that robust anhydrous phases may remain unaltered, others, such as the fine-grained porous matrix, may undergo changes in which precipitated minerals decrease porosity

(CONSOLMAGNO *et al.*, 1998). Evaporite minerals have also been noted on meteorite surfaces and are attributed to element mobility as terrestrial water reacts with the meteorite. The dissolved ions precipitate the elements on meteorite surfaces with evaporation. Reactions of meteoritic minerals with terrestrial water and gases also may occur.

The goal of this project is to examine how terrestrial alteration affects both carbon and oxygen isotopes of meteoritic carbonates. Studies of this nature have been undertaken with ALH84001, the Martian meteorite some suspect as containing evidence of life, and other Antarctic meteorites (BREARLEY *et al.*, 1999a; JULL *et al.*, 1995; JULL *et al.*, 1997). A study of paired meteorites that can preserve changes as they occurred, however, has not been undertaken. A goal of this study is to evaluate the combined carbon and oxygen isotope geochemistries in a way that will allow better interpret data for meteorite finds. If terrestrial alteration trends can be evaluated in a fashion that allows pre-weathered compositions to be estimated, the vast Antarctic meteorite collection should become more useful to researchers.

## **Chapter 2: Terrestrial Alteration of a suite of Antarctic CM2**

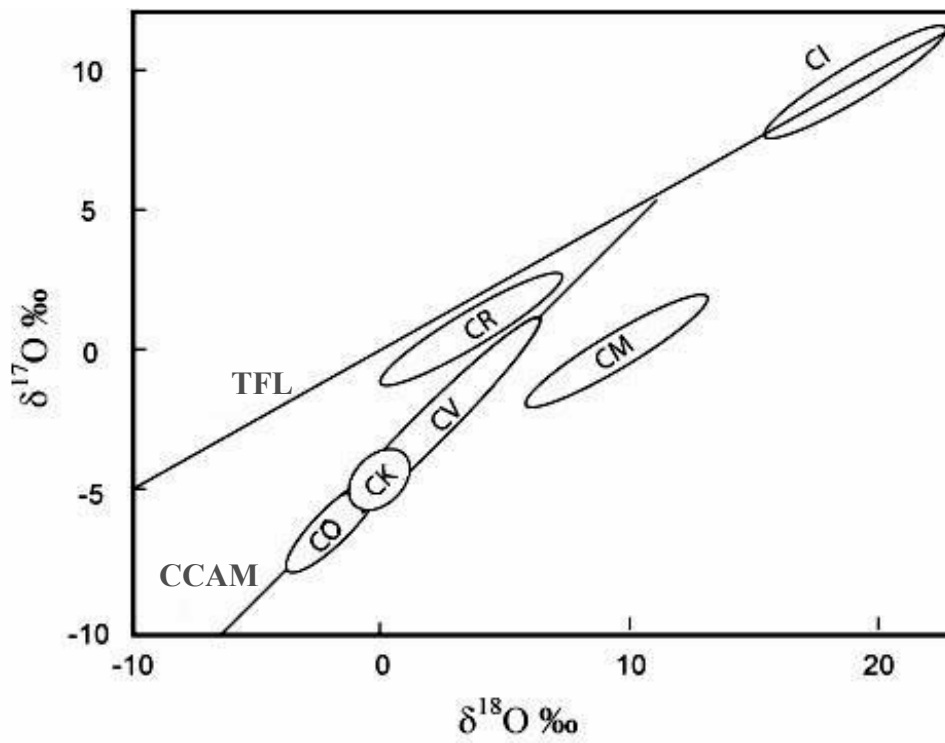
### **chondrite meteorites**

## 2.1 Introduction

Studies by Clayton and Mayeda (1984, 1999) have documented the heterogeneity of oxygen isotopic compositions among CM2 carbonaceous chondrites and their components. Anhydrous minerals within CM2 carbonaceous chondrites fall along the Carbonaceous Chondrite Anhydrous Minerals line (CCAM), an array with a slope of approximately 1 on a plot of  $\delta^{18}\text{O}$ - $\delta^{17}\text{O}$ , which is interpreted to reflect isotopic mixing between original silicate oxygen with nebular or planetesimal water oxygen (Fig. 3) (CLAYTON AND MAYEDA, 1999). In CM2 chondrites, hydrated minerals and matrix phases define oxygen isotope arrays that are interpreted to reflect mass-dependent fractionations produced in parent bodies as a result of low temperature reactions and isotope exchange involving water and silicate. It has also been established that the oxygen isotopic compositions of some matrix phases preserve information about the isotopic evolution of the fluid phase during these asteroidal alteration events (AIRIEAU *et al.*, 2005; BENEDIX *et al.*, 2003; ROWE *et al.*, 1994; YOUNG *et al.*, 1999).

Calcite, accompanied by accessory dolomite and aragonite, is the dominant carbonate mineral phase of extraterrestrial origin in most CM2 chondrites (BARBER, 1981; BENEDIX *et al.*, 2003; BREARLEY and JONES, 1998; JOHNSON and PRINZ, 1993; RICIPUTI *et al.*, 1994). Carbonate minerals occur primarily as isolated grains in the meteorite matrix; a few grains are reported to occur as inclusions, crosscutting veins, and as replacement minerals in chondrules (BENEDIX *et al.*, 2003; FUCHS *et al.*, 1973). Carbonate grains are thought to form predominantly by precipitation from fluids during low temperature alteration in the parent body (FREDRIKSSON and KERRIDGE

**Figure 3.** Oxygen isotope signatures of carbonaceous chondrites by type. The TFL is the terrestrial fractionation line and the CCAM is the carbonaceous chondrite anhydrous mineral mixing line. After Brearley and Jones, 1998.



(1988). The low Mg (~0 mole %), Mn (~0 mole%) and Fe (~0.5 mole %) content combined with high  $^{18}\text{O}$  content relative to other phases forms the basis for the assignment of calcite as a low temperature phase (JOHNSON and PRINZ, 1993). These impurity solubility constraints point to a temperature of formation  $\leq 250^\circ\text{C}$  (JOHNSON and PRINZ, 1993), and oxygen isotope modeling of calcite precipitation at equilibrium conditions further narrows the formation temperatures ( $T_f$ ) ( $0^\circ\text{C} \leq T_f \leq 25^\circ\text{C}$ ) (BENEDIX *et al.*, 2003; CLAYTON and MAYEDA, 1984).

Riciputi *et al.* (1994) calculated the trace element composition (Fe, Mg, Mn, Sr, Na, B, and Ba) of fluids in equilibrium with calcite and dolomite in CM2 chondrites and noted that two separate source brines were necessary for precipitation of the two species. Riciputi and coworkers also suggested that calcite precipitated before dolomite during the final vein-infilling of the CM2 parent body. Aragonite, as noted by Barber (1981), is thought to have formed as a metastable phase. Aragonite is marked by less regular crystals than calcite and possess chemical compositions suggesting its formation post-dates calcite formation (Riciputi *et al.* 1994).

Experimental studies of oxygen isotope exchange between calcite grains and water suggest that exchange, barring re-precipitation, is slow (FARVER, 1994; LABOTKA *et al.*, 2000), allowing calcite grains to preserve oxygen isotope compositions that can provide insights about the CM2 parent body fluids (BENEDIX *et al.*, 2003; CLAYTON and MAYEDA, 1984). Clayton and Mayeda (1984) argued that the  $\Delta^{17}\text{O}$  of Murchison carbonates and matrix indicated that they precipitated in equilibrium with the parent-body fluid. Benedix *et al.* (2003) also argued that carbonates from Murchison, Murray, Mighei, Nogoya, and Cold Bokkeveld

precipitated in equilibrium with CM2 parent-body fluids, but the isotopic composition of this fluid had evolved to a greater extent by the time that the matrix had completely formed.

Polar and arid deserts provide climates lacking in liquid water, so chemical erosion is reduced, allowing for the preservation and recovery of a large number of meteorites (BLAND *et al.*, 2000). Antarctic ice flow and sublimation concentrate meteorites in well-defined locations, and these meteorites represent a valuable resource for studies of extraterrestrial processes (CASSIDY *et al.*, 1992). Even though cold temperatures reduce weathering, Antarctic meteorite collectors have noted liquid water on top of and immediately below the stones as they lay on the ice (HARVEY, 2003). Schultz (1986) tracked the temperature changes of a 310 g Allende sample placed upon the ice at Allan Hills and noted that when the wind dropped, the temperature within the meteorite rose above freezing—even though the ambient air temperature remained below  $-10^{\circ}\text{C}$ . In many cases, meteorites absorb sufficient summer solar radiation to become warm enough to melt surrounding ice, and several detailed evaluations of Antarctic meteoritic carbonates show that weathering can affect carbonate geochemistry by dissolution-precipitation both before and after ice burial (JULL *et al.*, 1988; JULL *et al.*, 1998; KOPP and HUMAYUN, 2003). In this study, we examine oxygen and carbon isotopes of carbonate minerals from a suite of paired CM2 chondrite meteorites from Elephant Moraine, Antarctica that are described in *The Meteoritical Bulletin* (GROSSMAN and SCORE, 1996). Paired meteorites share petrographic and chemical characteristics that suggest they derive from a single meteorite that broke up upon entry into Earth's atmosphere and

comprise shared pre-terrestrial histories that can be used to form a baseline for evaluating terrestrial alteration. A goal of our study was to evaluate the differential signature that terrestrial weathering imparts to meteorite finds, and thus to reconstruct a geochemical path back to unaltered materials.

## **2.2 Analytical Procedures**

### **2.2.1 Electron Microscopy**

We used scanning electron microscopy (SEM) to study calcite morphology and petrography. Because mineral grains, especially in the phyllosilicate matrix, are very small, element mapping along with SEM imaging often are most efficient tools meteoriticists use to study petrography of carbonaceous chondrites. Thick sections of samples EET96006, EET96016, EET96017, and EET96019 from the U.S. Antarctic collections were analyzed using the JEOL JXA-8900 electron probe microanalyzer (EPMA) at the Center for Microscopy and Microanalysis at the University of Maryland. The sections were too thick and the matrix too fine-grained, however, for transmitted light microscopy. Sections were carbon coated using standard thermal evaporation techniques, with a carbon coat thickness of  $\sim 300\text{\AA}$ . Samples were analyzed with an electron beam accelerated with a voltage of 15 keV, a cup current of 10 nA, and a beam diameter of 1  $\mu\text{m}$ . Samples were analyzed for Ca, Mg, Sr, Mn and Fe abundances (peak and background). Raw x-ray intensities were corrected using a CIT-ZAF algorithm: samples were initially assumed to be pure  $\text{CaCO}_3$ , and we assumed that the materials contained 44%  $\text{CO}_2$  (this was later reevaluated based on the cation chemistry, and found to have little effect on the concentrations reported in Table 1).

No.	SrO	MnO	MgO	FeO	CaO	CO <sub>2</sub>	Total
Matrix Calcites							
7	0.11	0.03	0.09	1.13	54.87	44	100.23
8	0.12	ND	0.87	0.67	59.98	44	105.65
9	0.07	0.03	0.06	0.69	58.00	44	102.85
10	0.17	0.19	6.06	29.18	14.04	44	93.64
11	0.10	ND	0.03	1.07	58.84	44	104.04
12	0.10	ND	0.02	0.97	58.46	44	103.56
13	0.10	ND	0.14	0.88	56.27	44	101.40
14	0.12	0.04	0.05	0.71	56.59	44	101.50
15	0.13	0.04	0.06	0.67	56.51	44	101.41
16	0.17	0.03	0.04	0.60	57.37	44	102.20
17	0.07	0.06	0.97	2.07	56.55	44	103.71
18	0.11	0.03	1.07	2.19	47.25	44	94.65
19	0.11	ND	0.21	0.35	41.99	44	86.68
20	0.06	0.04	0.90	2.13	49.72	44	96.84
21	0.16	0.05	0.60	1.71	52.29	44	98.80
22	0.13	0.05	1.69	2.39	51.66	44	99.92
23	0.12	0.07	1.10	1.77	51.87	44	98.94
24	0.06	0.04	0.28	1.12	53.50	44	99.00
25	0.12	ND	0.28	0.86	55.09	44	100.36
26	0.11	0.20	0.55	1.68	55.12	44	101.66
27	0.16	0.10	1.09	5.28	47.31	44	97.95
28	0.12	0.09	0.67	2.85	51.85	44	99.57
29	0.12	0.11	0.36	0.99	52.97	44	98.56
30	0.06	0.15	0.53	1.69	52.69	44	99.12
31	0.10	0.06	0.29	0.92	54.04	44	99.42
32	0.13	0.06	0.49	1.32	52.31	44	98.32
33	0.06	0.21	0.64	1.70	55.19	44	101.80
34	0.07	0.07	0.21	0.84	56.38	44	101.57
35	0.10	0.06	0.24	4.99	41.44	44	90.83
36	0.10	0.35	2.13	3.10	49.22	44	98.91
37	0.04	0.21	17.47	27.68	4.21	44	93.62
42	0.06	0.14	2.42	11.14	39.85	44	97.61
43	0.14	0.07	0.20	0.66	58.64	44	103.72
44	0.08	0.13	0.44	0.65	58.63	44	103.93
Vein carbonates (hydrated Mg-carbonates)							
38	0.02	ND	38.51	2.05	0.05	44	84.64
39	0.07	ND	36.43	0.55	0.05	44	81.09
40	0.04	ND	4.60	0.42	31.52	44	80.59
41	0.11	0.19	13.06	38.77	0.43	44	96.56
45	0.05	ND	29.13	1.41	0.10	44	74.71
46	0.04	0.03	31.07	2.62	0.08	44	77.84
47	0.06	0.11	23.81	16.49	0.16	44	84.62
48	0.17	0.20	34.43	22.73	0.36	44	101.89
49	ND	0.03	44.71	0.56	ND	44	89.31
50	0.06	0.06	33.23	5.44	0.11	44	82.90

Table 1. Composition of carbonates within EET96006 (Wt. %). Because of the possible variations in hydrated carbonates, no empirical formula has been calculated. CO<sub>2</sub> was set at 44 wt%. Water in vein carbonates varied widely and was surmised from deviations less than 100% in total counts of all measured oxides.

## 2.2.2 Isotopic Analysis

Sample chips (~1 g) of EET96006, EET96016, EET96017, EET96018, EET96019, and EET96029 from the U.S. Antarctic collections were prepared for bulk-carbonate and whole-rock isotopic analysis. Each sample was crushed with a steel percussion mortar and the crushed material was subdivided for bulk-carbonate (~0.5 g) and for laser fluorination (~10 mg) analyses.

Isotopic ratios are reported using standard delta notation:

$$\delta^{18}\text{O} = 1000 * [({}^{18}\text{O}/{}^{16}\text{O})_{\text{sample}} / ({}^{18}\text{O}/{}^{16}\text{O})_{\text{SMOW}} - 1];$$

$$\delta^{17}\text{O} = 1000 * [({}^{17}\text{O}/{}^{16}\text{O})_{\text{sample}} / ({}^{17}\text{O}/{}^{16}\text{O})_{\text{SMOW}} - 1];$$

$$\delta^{13}\text{C} = 1000 * [({}^{13}\text{C}/{}^{12}\text{C})_{\text{sample}} / ({}^{13}\text{C}/{}^{12}\text{C})_{\text{VPDB}} - 1]; \text{ and}$$

$$\delta^{14}\text{C} = 1000 * [({}^{14}\text{C}/{}^{12}\text{C})_{\text{sample}} / ({}^{14}\text{C}/{}^{12}\text{C})_{\text{SRM 4990C}} - 1],$$

where the subscripts refer to the reference materials (Standard Mean Ocean Water (SMOW), PeeDee belemnite (VPDB), and SRM 4990C). We report  $\Delta^{17}\text{O}$  using

$$\Delta^{17}\text{O} = \delta^{17}\text{O} - 1000 ((1 + \delta^{18}\text{O}/1000)^{0.5247} - 1).$$

The term “ $\delta^{14}\text{C}$ ” is not normalized and does not account for  $^{14}\text{C}$  decay in the standard or the addition of nuclear-bomb produced  $^{14}\text{C}$  incorporated into the French beets from which the standard (SRM 4990C) was made (RASBERRY, 1983; STUIVER and POLACH, 1977). In usage,  $^{14}\text{C}$  isotopes are normalized to a 1950 (pre-bomb) ratio and

pegged to the sample's  $\delta^{13}\text{C}_{\text{VPDB}}$  value. This normalized term,  $\Delta^{14}\text{C}$ , is calculated as follows:

$$\Delta^{14}\text{C} = \delta^{14}\text{C} - 2 * (\delta^{13}\text{C}_{\text{VPDB}} + 25) * (1 + \delta^{14}\text{C}/1000).$$

A simpler term used within this paper is the percentage of modern  $^{14}\text{C}$  within the sample. This term, FMOD  $^{14}\text{C}$  is defined as

$$\text{FMOD } ^{14}\text{C} = ^{14}\text{C}/^{12}\text{C}_{\text{sample}} / (^{14}\text{C}/^{12}\text{C})_{\text{SRM 4990C}}.$$

Uncertainties for all carbon and oxygen isotope analyses are given within the results (Table 4).

Approximately 1.5 mg of each sample was analyzed for its whole-rock oxygen isotopic composition using laser fluorination techniques (SHARP, 1990). The laser fluorination manifolds at UCSD use 25 W Synrad  $\text{CO}_2$  lasers and  $\text{BrF}_5$ . Molecular oxygen produced during the fluorination reaction is purified by passing it through liquid nitrogen-cooled traps ( $-196^\circ\text{C}$ ), by capturing it onto 13X molecular sieve and then releasing it from this sieve at  $-110^\circ\text{C}$  and subsequently capturing it on a second 13X-molecular sieve trap. These steps tend to capture condensable gases, such as water vapor and allow only oxygen to be collected in the final sieve trap. The purified oxygen (2.68 to  $27.33\mu\text{mol}$ ) is introduced to the mass-spectrometer by warming the second molecular sieve trap to  $80^\circ\text{C}$ . Oxygen isotopic determinations were made using a dual inlet Finnigan MAT251 mass spectrometer at UCSD. Uncertainties ( $1\sigma$ )

for individual isotopic analyses are estimated to be  $\pm 0.2$ ,  $0.1$ , and  $0.05$  ‰ (SMOW) for  $\delta^{18}\text{O}$ ,  $\delta^{17}\text{O}$ , and  $\Delta^{17}\text{O}$ , respectively on the basis of repeated analyses of UWG2. The variability among duplicate analyses of individual sample aliquots may be larger because they may consist of mixtures of materials with a diverse range of isotopic compositions. Data are reported relative to Standard Mean Ocean Water (SMOW) by assuming a mass-dependent  $\delta^{18}\text{O}$  value of  $5.8$ ‰ for UWG-2 garnet standard analyzed concurrently with the meteorite samples.

We extracted  $\text{CO}_2$  from carbonate contained in crushed samples of the meteorites using a side-arm reaction flask of the design used by McCrea (1950). Five cc of 100% phosphoric acid ( $\rho = 1.897$  g/cc) were transferred by pipette into the side arm of this flask, the flask was assembled, and evacuated for at least three hours. Each flask was then closed, removed from the vacuum manifold, and placed in a  $25^\circ\text{C}$  water bath for a twenty-four-hour leak test. After the leak test, the sample tubes were returned to the water bath for 30 minutes before tilting the flask to introduce the acid to the meteorite powder. Phosphoric acid reacts with carbonate in the sample to release carbon dioxide. Reactions of phosphoric acid with other components in the sample produce other gases (e.g., hydrogen sulfide is produced by reaction of monosulfides such as troilite ( $\text{FeS}$ )). Samples were left to react with phosphoric acid at  $25^\circ\text{C}$  overnight.  $\text{H}_2\text{S}$  and  $\text{CO}_2$  were purified by passing them through a series of glass traps cooled with ethanol- $\text{N}_2$  (l) slush at  $-90^\circ\text{C}$ . Carbon dioxide and hydrogen sulfide were frozen to a stainless-steel sample tube using liquid nitrogen, which was kept at liquid nitrogen temperatures and transferred to a second manifold that is attached to a Varian 3600 gas chromatograph for separation and purification of the

gases. The Varian 3600 gas chromatograph is equipped with a thermal conductivity detector and an 8 foot long 1/8 inch diameter Haysep-Q packed column was used for the separations (CASSIDY *et al.*, 1992; FARQUHAR and THIEMENS, 2000; FARQUHAR *et al.*, 1998). The side-arm flask was then prepared for extraction of a high-temperature fraction. The ethanol-N<sub>2</sub> (l) slush-cooled traps on the manifold were thawed, evacuated, and then refrozen with liquid nitrogen. The acid/meteorite powder mix in the side-arm reaction flask was warmed by raising a silicon-oil bath heated to 150°C around the base of the side arm flask. The reaction at 150°C similarly produces water, carbon dioxide, and hydrogen sulfide, which are trapped in the liquid nitrogen-cooled traps along with non-condensable gases. The progress of the reaction was monitored for three hours and the manifold was evacuated of non-condensable gases when the pressure exceeded 500 millitorr. At the end of the reaction, the vacuum manifold was isolated, and the carbon dioxide and hydrogen sulfide were separated from water-ice condensed in the traps by replacing the liquid nitrogen dewars used to cool the traps with dewars filled with an ethanol-N<sub>2</sub> (l) slush (-100°C) and by capturing the CO<sub>2</sub> and H<sub>2</sub>S in a stainless steel sample tube which was subsequently transferred to the Varian GC manifold for separation of carbon dioxide and hydrogen sulfide. The two purified CO<sub>2</sub> samples from each extraction were then split.

Half of the carbon dioxide extracted from each sample was transferred to a nickel reaction vessel along with a 1000-fold excess amount of purified BrF<sub>5</sub>. The reaction vessels were sealed and heated for 45 hours at 800°C to convert the carbon dioxide to molecular oxygen gas and carbon tetrafluoride. O<sub>2</sub> and CF<sub>4</sub> (g) were separated from residual reagent by trapping the reagent in a liquid nitrogen cooled

trap, and subsequently condensing the O<sub>2</sub> and CF<sub>4</sub> (g) into a trap filled with 13X molecular sieve cooled with liquid nitrogen. This trap was subsequently isolated and warmed to -116°C for 60 minutes to liberate O<sub>2</sub> and retain CF<sub>4</sub> (g). The molecular oxygen was analyzed for its isotopic composition at UCSD using a Finnigan MAT 251 mass spectrometer.

The other half of each CO<sub>2</sub> sample was sealed in a Pyrex break seal and reserved for carbon isotopic analysis at the University of Arizona Accelerator Mass Spectrometer laboratory (AMS lab). Each sample tube was broken under vacuum to release its content and introduce it into a manifold. Released carbon dioxide gas was passed through three -90°C slushes (ethanol and N<sub>2</sub> (l) mix) to remove ambient water and transferred to a sample tube cooled with liquid nitrogen. The sample was then introduced to a VG Isotech Dual Inlet Isotope Ratio mass spectrometer for analysis of δ<sup>13</sup>C and δ<sup>18</sup>O. Unprocessed CO<sub>2</sub> was recaptured from the mass spectrometer cryogenically back into the sample tube. Next, small aliquots of iron were measured and the CO<sub>2</sub> gas was reduced to form graphite via the method of Slota (1987): A heated Zn finger (500°C) was used to convert CO<sub>2</sub> to CO and the iron (750°C) further reduces the CO to carbon vapor. The vapor then precipitated to graphite in a cool zone (500°C) adjacent to the iron. This graphite, which is the form of carbon that is most efficiently ionized, was pressed into pellets and loaded into a multiple sample holder along with oxalic acid standards. A cesium ion beam struck the graphite and ionized carbon was ejected into the AMS.

Because <sup>14</sup>C is so rare (1/10<sup>12</sup> of carbon in modern samples) and <sup>14</sup>N so common, a particle accelerator is ideal to ensure complete separation of <sup>14</sup>C for

analysis. We used a NEC 3MV accelerator mass spectrometer for these analyses. See Donahue (1995) for an excellent summary of how the University of Arizona AMS is operated and Donahue *et al.* (1990) for additional insights into how measurements were taken.

### 2.2.3 Treatment of Isotopic Data

We evaluated relationships between different isotopic data sets using a Monte-Carlo (bootstrap) analysis of uncertainties. A series of 1000 synthetic sets of data of the same size as the measured dataset were constructed from a random selection of subsets grouped according to sample split (e.g.,  $\delta^{18}\text{O}$ ,  $\delta^{17}\text{O}$ ,  $\delta^{13}\text{C}$ , and FMOD<sup>14</sup>C were all grouped by sample split). The same procedure was used to construct a synthetic dataset for the Benedix *et al.* (2003) data. The synthetic datasets were then used for regression of slopes and intercepts between different types of isotopic data and to evaluate the certainty with which these values can be determined.

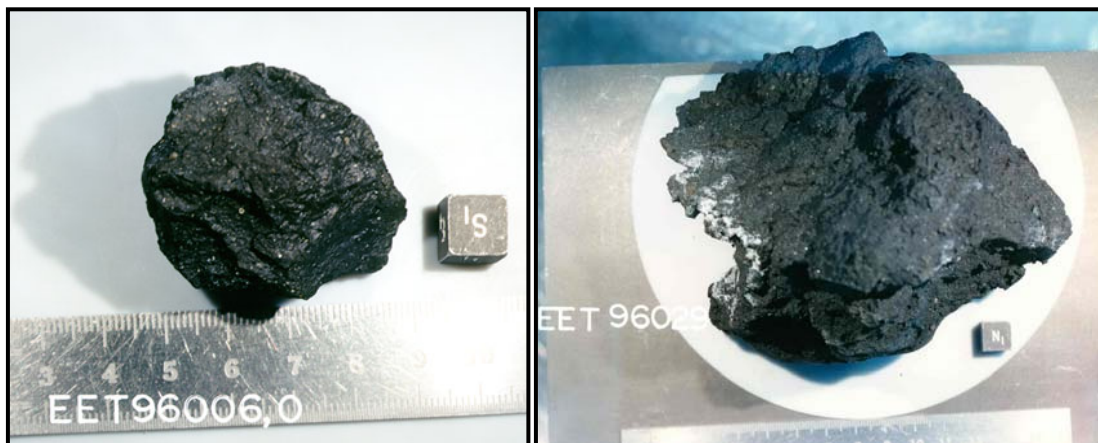
## 2.3. Samples

The samples examined here included EET96006, EET96016, EET96017, EET96019, and EET96029, which are all listed as paired with EET96005 in The Antarctic Meteorite Newsletter (LINDSTROM *et al.*, 1998). Lindstrom *et al.* (1998) distinguished EET96029 separately and placed its pairing as more tentative. Table 2 and Figure 4 give more information of the description of the EET96005 group including the samples in this study. Meteoritic fragments are assigned a relationship

**Table 2:** Description of EET-paired meteorites (from Lindstrom (1998) and Benoit *et al.* (2000)). Meteorite pairings are based upon petrographic textures and proximity of finds. Weathering grade is based on the following: A = minor rustiness, B = moderate rustiness, C = severe rustiness and e = evaporites visible. Fracturing is also based upon an ABC scale. The score represents the likelihood the pairing is correct: >90 = likely, 80-90 = probable, 70-80 = possible, 50-70 = potential, and <50 = candidate or unlikely. \* EET96029, score notwithstanding, may not be paired, as discussed in Lindstrom (1998) and further within the text.

Sample	Original Mass (g)	Weathering	Fracturing	paired?	basis	score
EET96006	42.15	Be	B	y	pet, geog	87.3
EET96016	132.14	Be	B	y	pet, geog	87.3
EET96017	19.92	Be	B	y	pet, geog	87.3
EET96018	5.89	Be	B	n	n/a	n/a
EET96019	18.87	Be	B	y	pet, geog	87.3
EET96029	843.29	A-B	B	y*	pet, geog	87.3

**Figure 4.** Photographs of intact EET96006 and EET96029. Both meteorites show white evaporites upon their surfaces. Photographs courtesy of Kevin Righter (Johnson Space Center, NASA)



on the basis of consistent petrologic characteristics and collection within a limited geologic proximity. Benoit et al. (2000) notes that it is easy to disprove paired meteorites, but hard to prove they actually had the same parent. For further tests of consistency, we evaluated the whole-rock oxygen isotopic ratios of the samples, as well as the oxygen and carbon isotopic abundances of carbonates to test the pairing assignments. The unrelated C2 meteorite EET96018 was also carried through all extractions for comparison.

## 2.4 Results

### 2.4.1 Petrography

Carbonate grains were identified in all thick sections of EET96006, EET96016, EET96017, and EET96019 and include calcium carbonate, dolomite and a hydrated magnesium carbonate. The carbonate grains in these meteorites take several different forms, and with the exception of two unusual isolated, subhedral 100  $\mu\text{m}$  calcium carbonate grains in EET 96006, all forms have been identified in all sections of these EET samples. EPMA analyses of selected carbonate grains are presented in Table 1. Types of carbonates found are:

1) *Subhedral grains unique to EET96006*: The two unusual calcium carbonate grains that are unique to EET96006 are intimately associated with forsterite that has minor inclusions of metallic iron (EDS analysis) (Fig. 5-a), and exhibit sharp contacts with the forsterite grains.

2) *Blocky calcium carbonate grains*: These calcium carbonate grains occur in isolation in the matrix of the paired samples. These grains are blocky, anhedral, and contain few inclusions. They also have rims of fine-grained material that may be tochilinite ((FeS)·(Mg,Fe)(OH)<sub>2</sub>) (Fig. 5b-d). Elemental analyses are presented in Table 1, numbers 7-22 and 42-44. These grains are generally less than 50µm in diameter.

3) *Mottled calcium-carbonate grains*: Grains occur in association within the fine-grained matrix (Fig. 5e-i). These grains have a mottled appearance when viewed by SEM and more diffuse, irregular grain boundaries. Elemental analyses are presented in Table 1, numbers 23-37, on a single large grain. These grains range from about 50 µm to 250 µm.

4) *Fracture and vein infill*: Carbonate minerals other than calcium carbonate have been identified only as infill of cross cutting fractures (Fig. 5j-n). Hydrated magnesium carbonate is by far the most common fracture infill mineral, while calcium carbonate and dolomite are less abundant. Carbonate-filled fractures cross-cut matrix mineral grains, including both morphologies of calcium carbonate grains just described. Elemental analyses are presented in Table 1, 38-40 and 45-51.

EPMA analyses of fracture and vein infill carbonates (Table 1) show low total counts (as low as 74 wt%). Because H and O detection via microprobe is limited, mineral hydration is the interpreted cause. Another contribution to the observed low totals may be a loose, porous structure (LEE and BLAND, 2004). Table 3 shows a few

of many possibilities for hydrated species of Mg-carbonates. A number of hydrated magnesium carbonates have been reported within and on Antarctic meteorites (JULL *et al.*, 1988; VELBEL *et al.*, 1991).

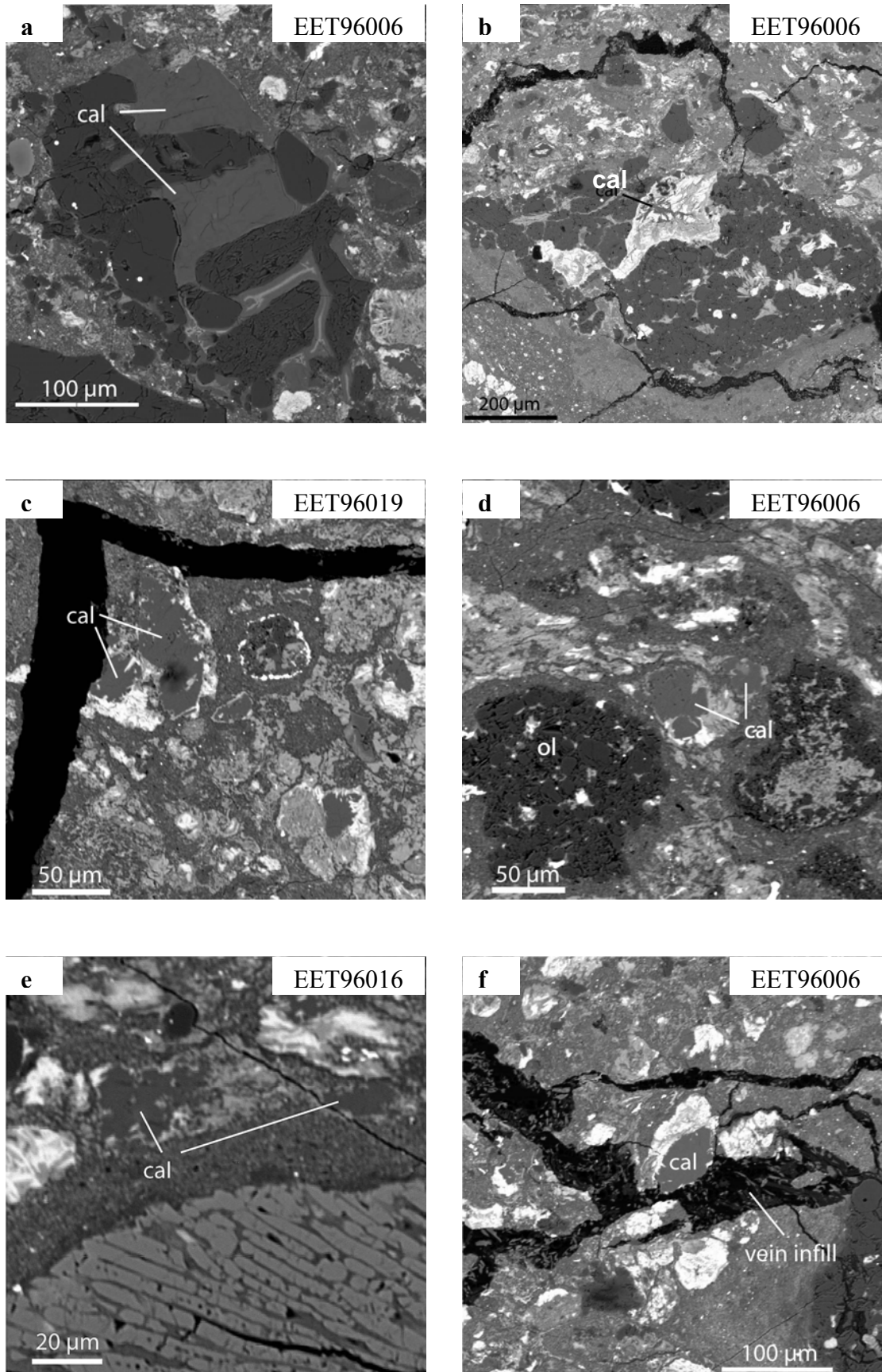
#### 2.4.2 Carbon and Oxygen Isotopic Data

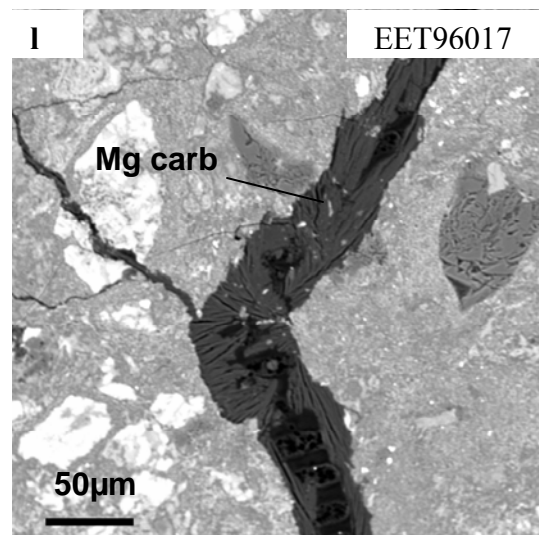
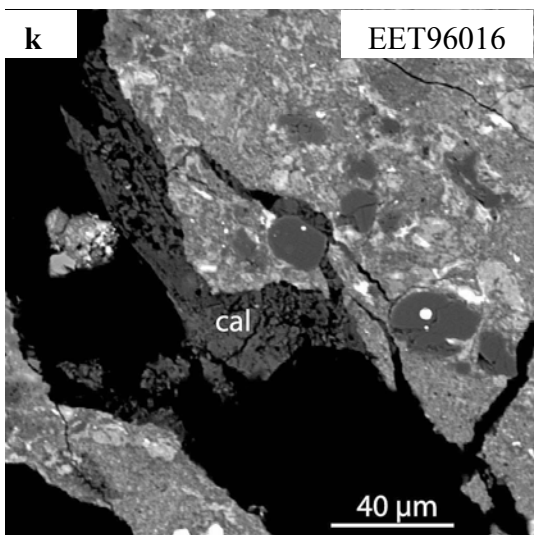
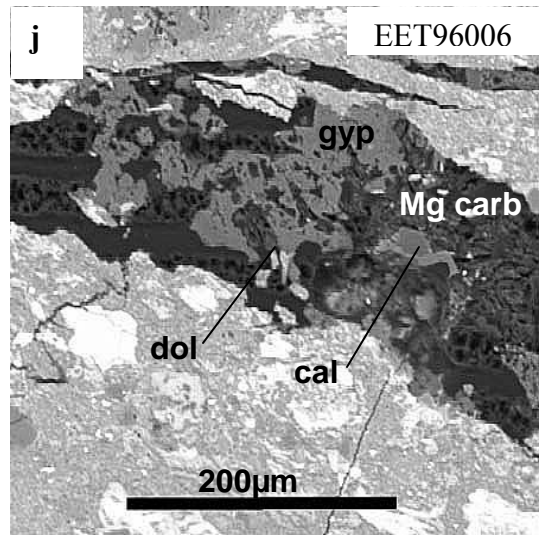
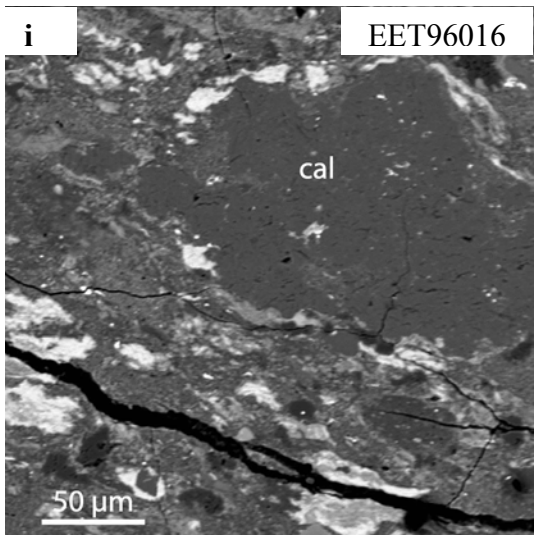
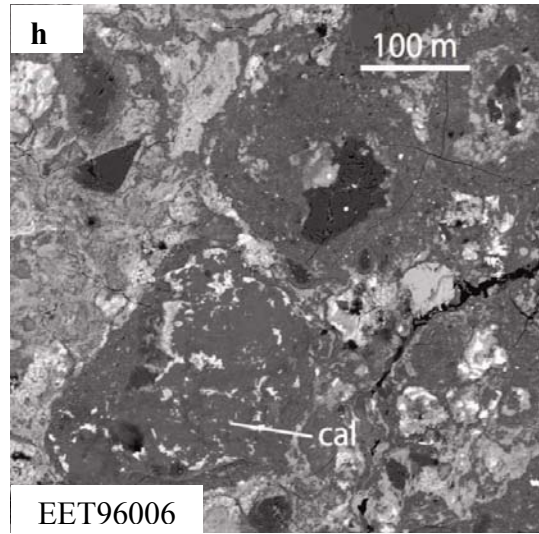
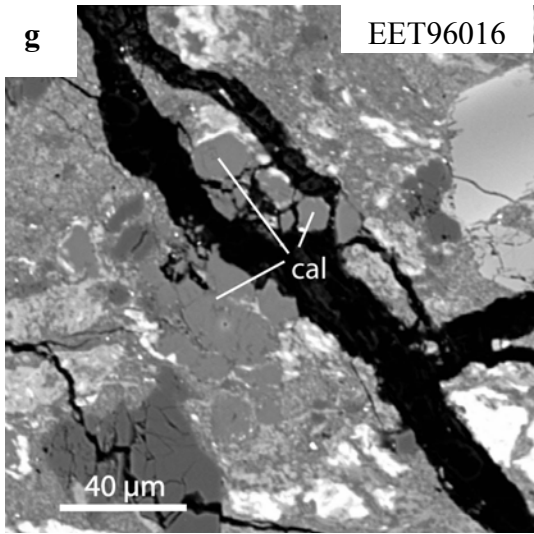
Table 4 presents data for yields of CO<sub>2</sub>,  $\delta^{13}\text{C}$ , FMOD<sup>14</sup>C,  $\delta^{17}\text{O}$ ,  $\delta^{18}\text{O}$ , and  $\Delta^{17}\text{O}$  for carbon dioxide extracted by acidification with phosphoric acid, and for whole-rock laser fluorination analyses of the samples examined in this study. The 25°C acidification for 18 hours (inferred to be calcium carbonate) yielded between 263 and 4140  $\mu\text{g/g}$  of CO<sub>2</sub> with  $\delta^{18}\text{O}$  of 22.08‰ to 27.78‰,  $\delta^{17}\text{O}$  of 9.22‰ to 13.28‰,  $\Delta^{17}\text{O}$  of -2.31 to -0.55‰,  $\delta^{13}\text{C}$  of 8.4‰ to 48.9‰, and FMOD<sup>14</sup>C of 0.08 to 0.45. Acidifications at 150 °C for 3 hours (inferred to be magnesium carbonates and dolomite) yielded between 769 and 4730  $\mu\text{g/g}$  of CO<sub>2</sub> with  $\delta^{18}\text{O}$  of 21.00‰ to 28.00‰,  $\delta^{17}\text{O}$  of 8.66‰ to 13.35‰,  $\Delta^{17}\text{O}$  of -2.31 to 0.49‰,  $\delta^{13}\text{C}$  of 12.7‰ to 49.4‰, and FMOD<sup>14</sup>C of 0.12 to 0.33. Whole-rock laser fluorination analyses yielded correlated  $\delta^{17}\text{O}$ ,  $\delta^{18}\text{O}$ , and  $\Delta^{17}\text{O}$  of 2.4‰ to 8.3‰, -2.6‰ to 2.3‰, -3.82‰ to -2.01‰ respectively. The isotopic compositions ( $\delta^{13}\text{C}$ , FMOD<sup>14</sup>C,  $\delta^{17}\text{O}$ ,  $\delta^{18}\text{O}$ , and  $\Delta^{17}\text{O}$ ) of CO<sub>2</sub> extracted from paired samples EET96006, EET96016, EET96017, and EET96019 appear to be correlated (Figs. 5-7). The most  $\Delta^{17}\text{O}$  negative calcium carbonate (EET96016, -1.31‰) also possessed the highest  $\delta^{13}\text{C}$  (34.54‰) and the lowest FMOD<sup>14</sup>C (0.1477). EET96019, with the least negative  $\Delta^{17}\text{O}$  (-0.55‰) has the lowest  $\delta^{13}\text{C}$  (8.37‰) and highest FMOD<sup>14</sup>C (0.4463) for calcium carbonate. Carbonate  $\Delta^{17}\text{O}$  values do not correlate with carbon-dioxide yields.

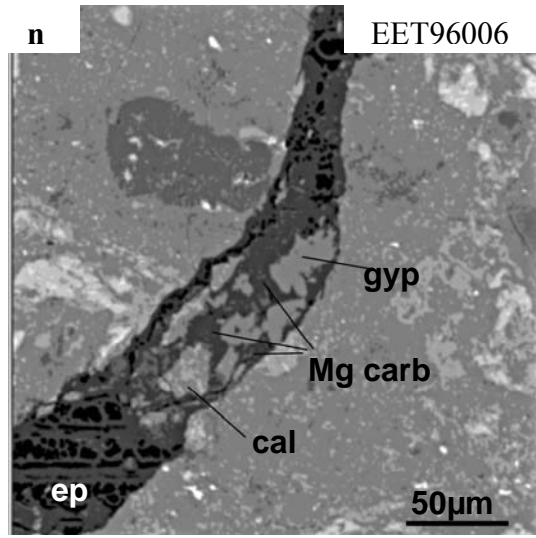
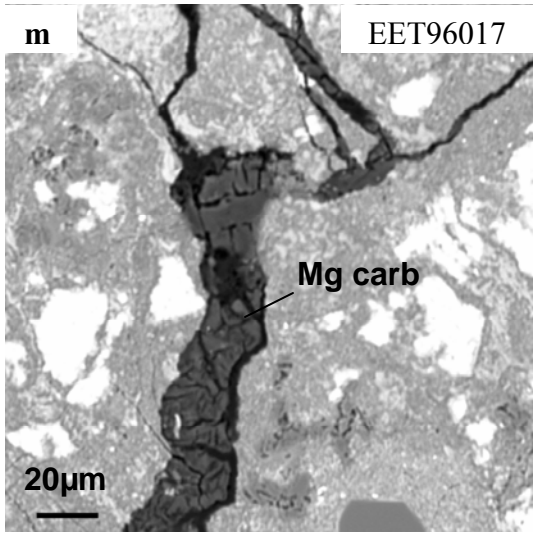
**Figure 5.** Examples of carbonates found within the EET paired suite. The descriptions of types of carbonates found here can be found in the text (Results, pg 12-13).

- a. Calcite with petrographically related olivine. This could be a clast of another meteorite. Unlike other calcites, there is no tochilinite or poorly characterized phyllosilicate (pcp) rim.
- b. Calcite (dendritic in appearance) surrounded by tochilinite and pcp within a chondrule.
- c. Typical blocky calcite (type 2) and veins
- d. Type 2 calcite between two chondrules
- e. Calcite outside of chondrule alteration rim. Calcites were often found just outside of alteration rims in wide arcs.
- f. Type 2 calcite, fracture (now filled) seems to have split the grain and tochilinite rim.
- g. Type 2 calcite, split by fracture
- h. Large mottled calcite (type 3) with inclusions of tochilinite
- i. Type 3 calcite
- j. Vein carbonates: dolomite, Mg-carbonate, and one dolomite area all evident. Gypsum also evident
- k. Vein calcite, near edge of section
- l. Vein Mg-carbonate
- m. Vein Mg carbonate
- n. Vein Mg-carbonate, gypsum, and what looks to be an isolated matrix (type 2) calcite

Figure 5







Mineral	formula	MgO	H <sub>2</sub> O	CO <sub>2</sub>	CaO	Fe <sub>2</sub> O <sub>3</sub>	FeO	total
Sergeevite	Ca <sub>2</sub> Mg <sub>11</sub> (CO <sub>3</sub> ) <sub>9</sub> (HCO <sub>3</sub> ) <sub>4</sub> (OH) <sub>4</sub> ·6(H <sub>2</sub> O)	33.9	13.78	43.75	8.58	-	-	100.01
MonohydroCalcite	Ca(CO <sub>3</sub> )·(H <sub>2</sub> O)	-	15.25	37.26	47.48	-	-	99.99
hydromagnesite	Mg <sub>5</sub> (CO <sub>3</sub> ) <sub>4</sub> (OH) <sub>2</sub> ·4(H <sub>2</sub> O)	43.09	19.26	37.64	-	-	-	99.99
giorgiosite	Mg <sub>5</sub> (CO <sub>3</sub> ) <sub>4</sub> (OH) <sub>2</sub> ·5(H <sub>2</sub> O)	41.5	22.26	36.25	-	-	-	100.01
Coalingite	Mg <sub>10</sub> Fe <sup>3+</sup> <sub>2</sub> (CO <sub>3</sub> )(OH) <sub>24</sub> ·2(H <sub>2</sub> O)	46.92	29.36	5.12	-	18.59	-	99.99
Barringtonite	Mg(CO <sub>3</sub> )·2(H <sub>2</sub> O)	33.49	29.94	36.57	-	-	-	100
Pyroaurite	Mg <sub>6</sub> Fe <sup>3+</sup> <sub>2</sub> (CO <sub>3</sub> )(OH) <sub>16</sub> ·4(H <sub>2</sub> O)	36.55	32.67	6.65	-	24.13	-	100
Sjogrenite	Mg <sub>6</sub> Fe <sup>2+</sup> <sub>2</sub> (CO <sub>3</sub> )(OH) <sub>14</sub> ·5(H <sub>2</sub> O)	37.45	33.38	6.82	-	-	22.25	99.9
brugnatellite	Mg <sub>6</sub> Fe <sup>3+</sup> (CO <sub>3</sub> )(OH) <sub>13</sub> ·4(H <sub>2</sub> O)	43.58	34.09	7.93	-	14.39	-	99.99
Artinite	Mg <sub>2</sub> (CO <sub>3</sub> )(OH) <sub>2</sub> ·3(H <sub>2</sub> O)	40.98	36.64	22.38	-	-	-	100
nesquehonite	Mg(HCO <sub>3</sub> )(OH)·2(H <sub>2</sub> O)	29.13	39.06	31.81	-	-	-	100
Lansfordite	Mg(CO <sub>3</sub> )·5(H <sub>2</sub> O)	23.11	51.65	25.24	-	-	-	100
Ikaite	Ca(CO <sub>3</sub> )·6(H <sub>2</sub> O)	-	51.92	21.14	24.96	-	-	98.02

**Table 3.** Various hydrated carbonates sorted by water content. Some, such as nesquehonite have been found upon weathered meteorites. Others have been observed on the surfaces of weathered basalts. All of these however could be represented within the paired EET meteorite filled veins. Oxide wt% source: [webminerals.org](http://webminerals.org)

**Figure 6.** Oxygen isotopic comparison between EET bulk carbonate and CM2 fall bulk carbonate.

- a. Comparison of EET CM2 finds (this study) with CM2 falls on a  $\delta^{18}\text{O}$  vs.  $\delta^{17}\text{O}$  three isotope diagram. The TFL is the terrestrial fractionation line and the CMCL is the observed CM2 chondrite line. The falls are data from Murchison, Murray, Mighei, Nogoya, and Cold Bokkeveld (Benedix *et al.*, 2003). The EET-line intersection with the TFL occurs at  $\delta^{18}\text{O} \approx 0\text{‰}$ , and the intersection with the CMCL line occurs at  $\delta^{18}\text{O} \approx +29.8\text{‰}$  and  $\Delta^{17}\text{O} \approx -1.25\text{‰}$ . These are inferred to represent the compositions of equilibrated carbonate with Antarctic water, and the extraterrestrial carbonate endmembers, respectively.
- b. An expansion of figure 2-a showing the projected intersection of the EET-line and the terrestrial fractionation line. The large error of intersection is due to a long extrapolation from the data while intersecting two sub-parallel lines. Note that carbonate in equilibrium ( $\delta^{18}\text{O}$ ) with the glacial EET ice would precipitate within the error envelope (FAURE *et al.*, 1993).
- c. Three oxygen isotope plot ( $\delta^{18}\text{O}$  vs.  $\delta^{17}\text{O}$ ) of EET find carbonates and that of CM2 falls of Benedix *et al.* (2003). The data have been linked to show 25°C and 150°C extractions (calcite and dolomite) of the same sample. Dolomite consistently plots lower ( $\delta^{18}\text{O}$  and  $\delta^{17}\text{O}$ ) than conjugate calcites.

Figure 6-a.

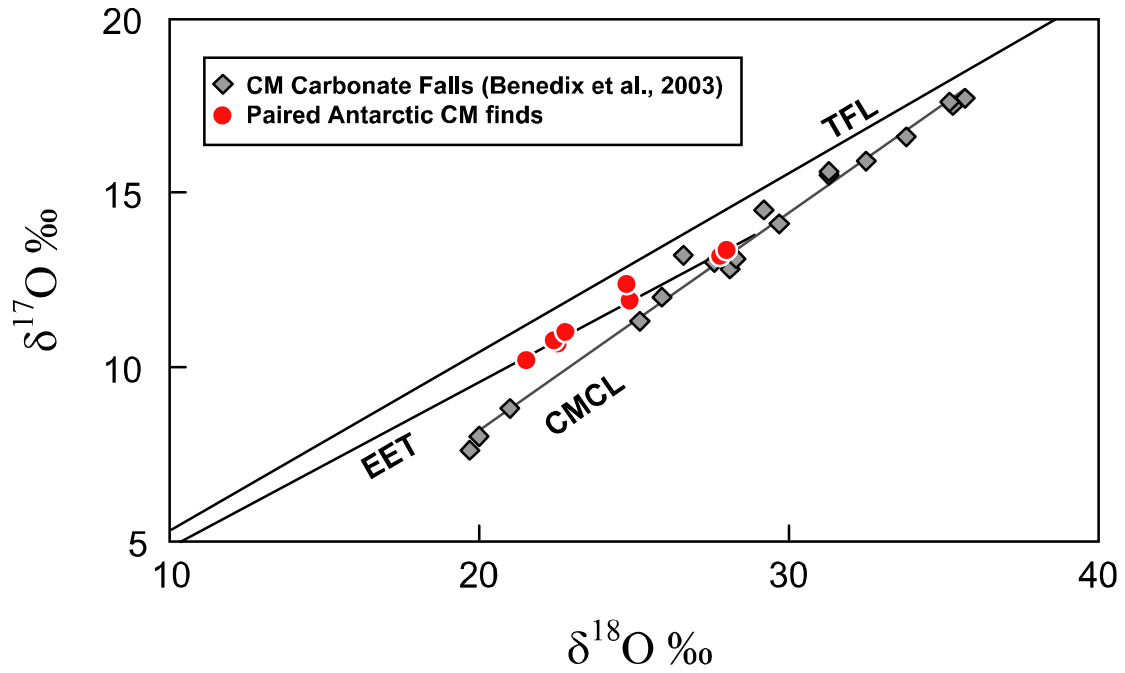


Figure 6-b.

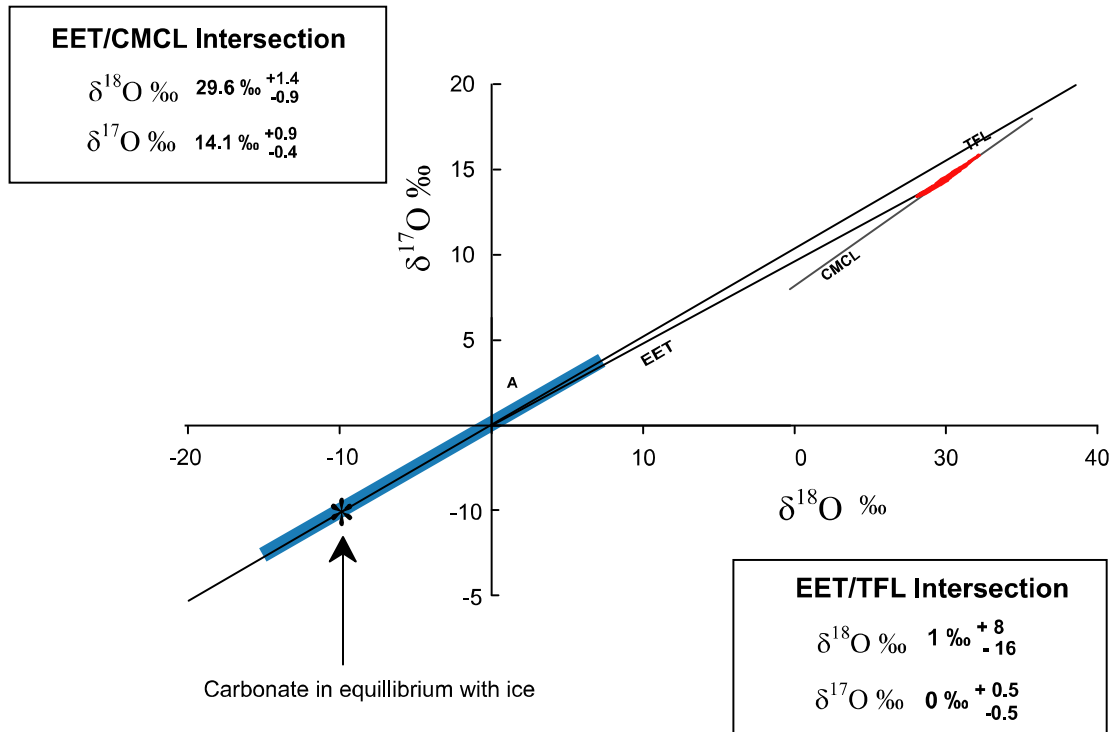
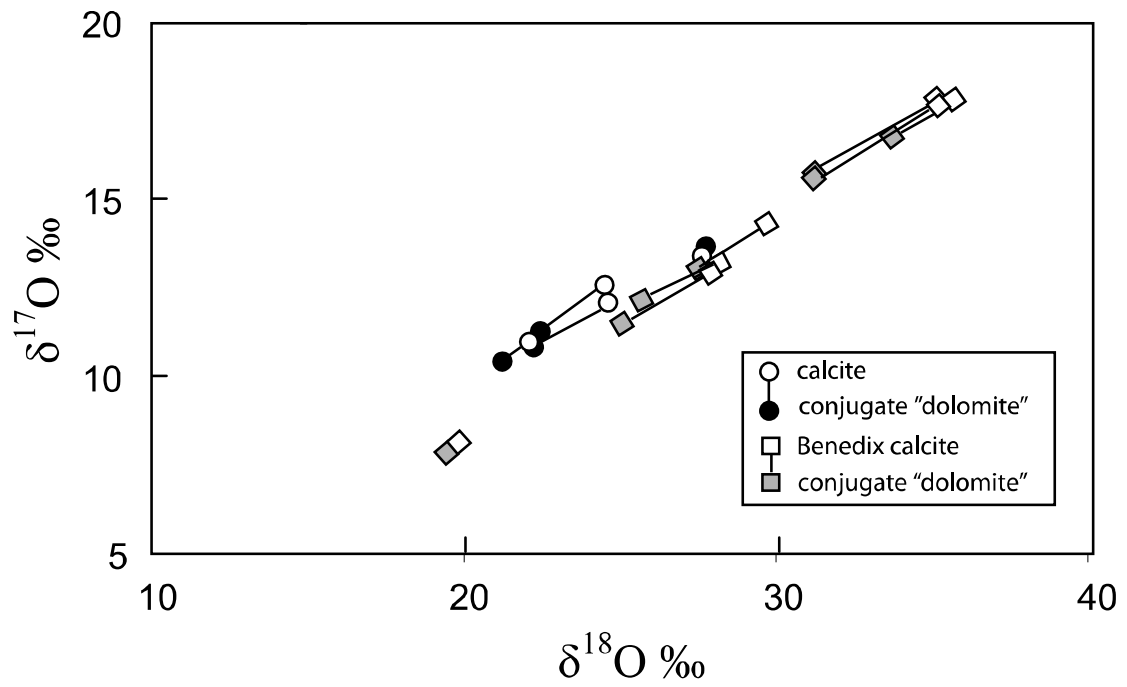
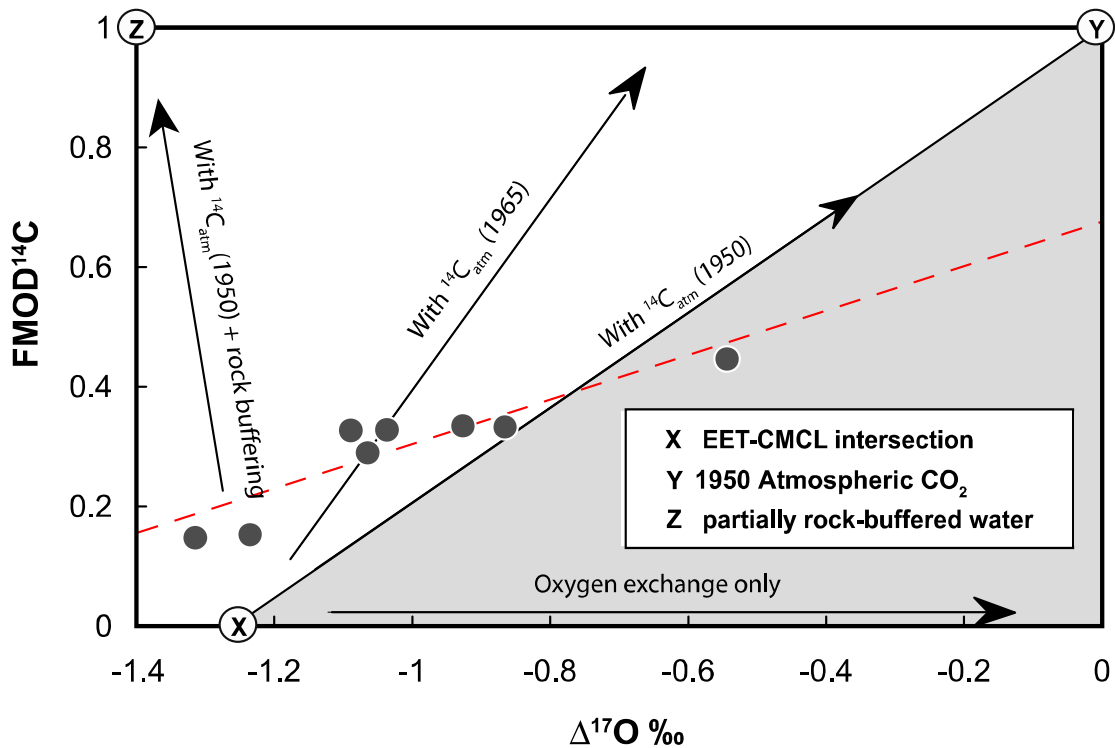


Figure 6-c.  
Comparison between calcite and dolomite.

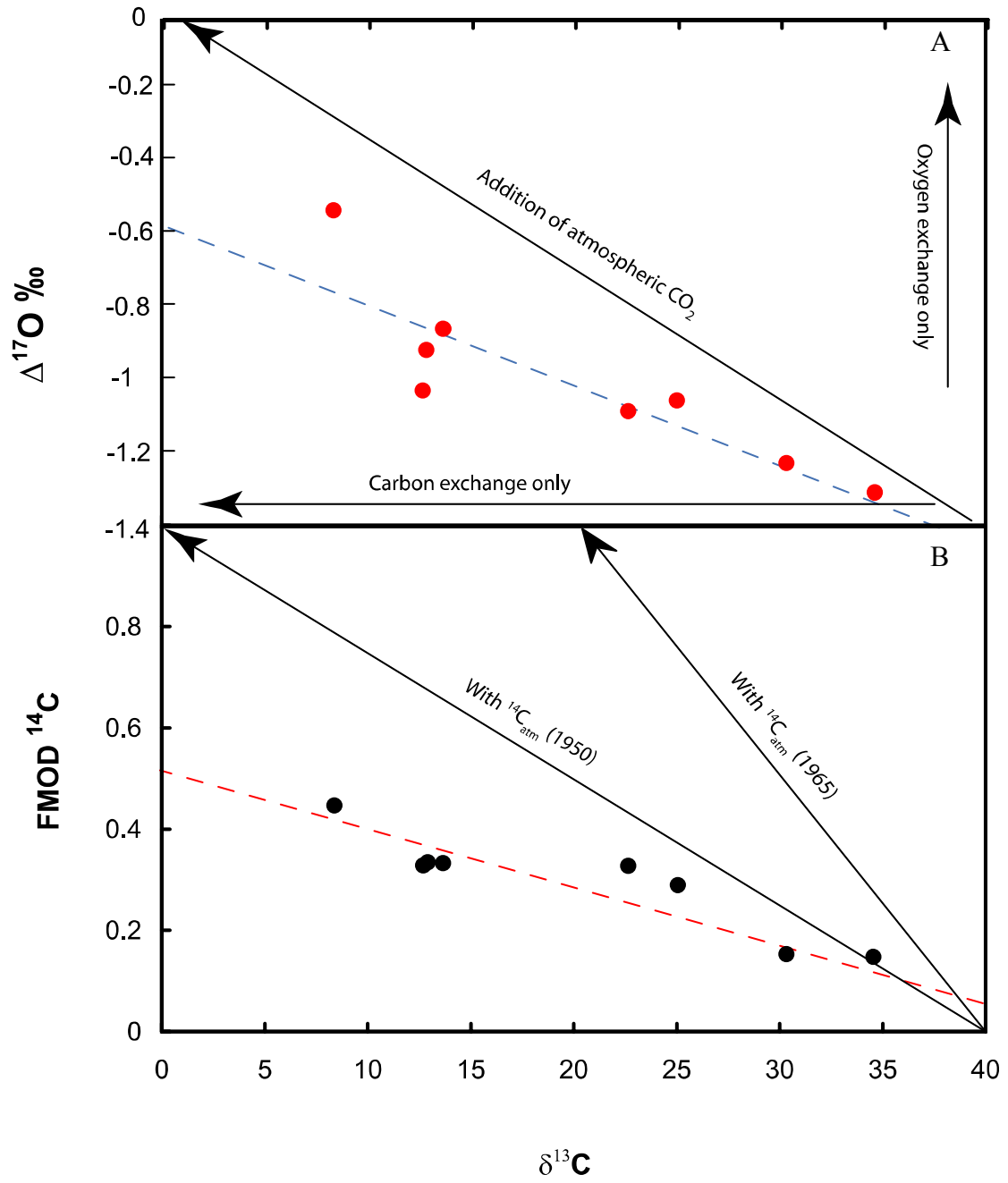


**Figure 7.** The fraction of modern  $^{14}\text{C}$  (FMOD $^{14}\text{C}$ ) vs.  $\Delta^{17}\text{O}$  in EET finds. Point X represents the EET-CMCL intersection (Fig. 6), which is the pre-terrestrial oxygen isotopic composition. Point Y is the calculated endmember if terrestrial carbonate incorporated 1950-level  $^{14}\text{C}$ . The vector marked “1965” gives a trend of terrestrial carbonate deposition if  $^{14}\text{C}$  was at 1965 levels (2-times 1950 concentration). Point Z gives a hypothetical trend of isotopic evolution with some rock buffering disturbing the terrestrial oxygen isotopic composition. The red line is the regression of the data, where the data form an array with a slope of  $0.40^{+0.11}_{-0.07}$  and a y intersection ( $\Delta^{17}\text{O} = 0\text{‰}$ ) at  $0.69^{+0.13}_{-0.05}\text{‰}$  (from FMOD $^{14}\text{C} = a * \Delta^{17}\text{O} + b$ ).



**Figure 8.** Plot of  $\delta^{13}\text{C}$  vs.  $\text{FMOD}^{14}\text{C}$  and  $\Delta^{17}\text{O}$ . Plot shows vectors of expected terrestrial alteration; however both data sets plot with shallower slopes than expected. The two plots show that an input of dead ( $^{14}\text{C}$  absent), negative  $\delta^{13}\text{C}$  carbon may be altering the isotopic composition of terrestrial carbonates. The regression (blue line) of Fig 4-a forms an array with a slope of  $-0.021_{-0.005}^{+0.006}$  and an intersection at  $-0.60_{-0.17}^{+0.13}$  (form  $\Delta^{17}\text{O} = a * \delta^{13}\text{C} + b$ ). The regression of the data in 4-b (red line) form an array with a slope of  $-0.010_{-0.001}^{+0.002}$  and an intersection at  $0.48_{-0.04}^{+0.03}$  (from  $\text{FMOD}^{14}\text{C} = a * \delta^{13}\text{C} + b$ ). Uncertainties are reported for the central 2/3 of the data.

Figure 8



## 2.5 Discussion

### 2.5.1 Pairing

The EET samples that were paired with EET96005 by Lindstrom (1988) had similar  $\Delta^{17}\text{O}_{\text{WR}}$  ( $-2.0\text{‰}$  and  $-2.6\text{‰}$ ) except EET96029, which possessed a  $\Delta^{17}\text{O}_{\text{WR}}$  that is significantly more negative ( $-3.8\text{‰}$ ) than the other paired EET samples. Lindstrom (1998) also classified EET96029 separately from the other paired samples because it was slightly less weathered (A/B compared to Be; see Table 1). Lindstrom *et al.* (1998) reported minor rust in all of the samples tentatively paired with EET960005 samples except EET96029. EET96029 is also the largest of the samples, 843.3 g compared to the range of 18.9-132.1 g for all other paired EET samples. EET96029 also yielded significantly less carbonate  $\text{CO}_2$  when acidified at  $25^\circ\text{C}$  ( $263\text{ }\mu\text{g/g}$ , Table 4). We suggest that uncertainties in the pairing of EET96029 with EET96005 are significant enough to warrant not including it in the data analysis presented below. Nonetheless, we recognize the possibility that our chip of EET96029 may not be representative of the bulk meteorite.

### 2.5.2 Carbonate Formation, Extraterrestrial and Terrestrial

Benedix *et al.* (2003) reported oxygen isotope data for carbonates from five CM2 chondrite falls (Murchison, Murray, Nogoya, Cold Bokkeveld, and Mighei). They argued for a relationship for these meteorites based on the oxygen isotope compositions of carbonates, their morphology, and the quantitative alteration grade of each. In addition, Benedix *et al.* (2003) described a variety of unusual carbonate texture in these falls:

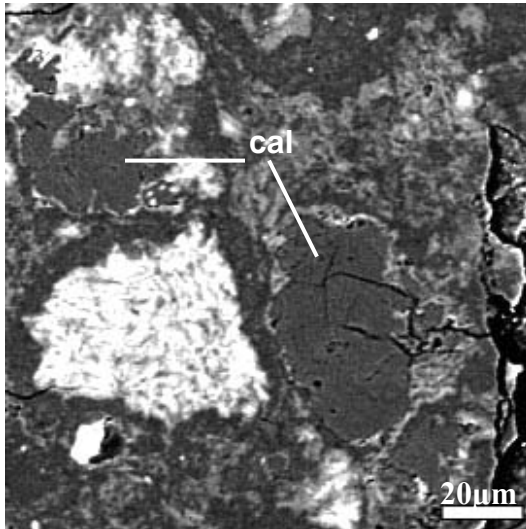
1. Isolated, inclusion-free, subhedral to subrounded, 20- to 50- $\mu\text{m}$  grains occurring in the matrix of Murchison and Murray,
2. rounded aggregates of calcite grains with included minerals such as olivine, pyroxene and sulfide that are interpreted to be replacement products of chondrules in Nogoya, and
3. features suggesting resorption in Cold Bokkeveld in the form of calcite grains that are surrounded by and in some cases invaded by altered material interpreted to be a fine-grained mixture of tochilinite and Fe-rich phyllosilicates.

These authors argued that the oxygen isotopic compositions of the carbonates preserved information about the compositions of coexisting fluids, which had equilibrated to variable degrees with silicate phases. The sequence of growth of carbonate minerals from aqueous fluids followed by exchange with the same fluids during low temperature protoplanetary alteration processes were interpreted by Benedix *et al* (2003) to be part of a continuum that occurred during the first hundred million years of solar system history and reflected solely extraterrestrial processes. A subsequent report (Benedix and Bland, 2004) introduced the possibility that some of the carbonate formation may have occurred after the meteorites arrived on Earth, but this suggestion remains to be established.

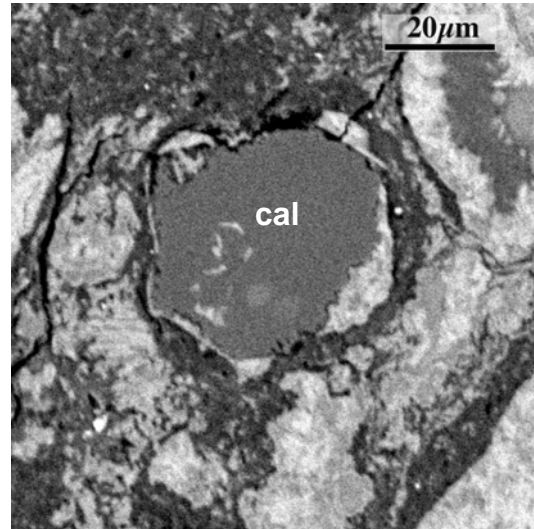
A number of prior studies have similarly addressed the issue of terrestrial versus extraterrestrial formation of carbonate, noting that many of the same processes involved in parent-body aqueous alteration also apply on Earth. While meteorite fracturing and subsequent infilling clearly occurs on the parent body, meteorite falls

**Figure 9.** Comparison of CM2 fall carbonates with those found in this study's EET paired set. The Murchison type 3 carbonates may or may not be related to EET type 3 (mottled) carbonates. However, they do have some similarities.

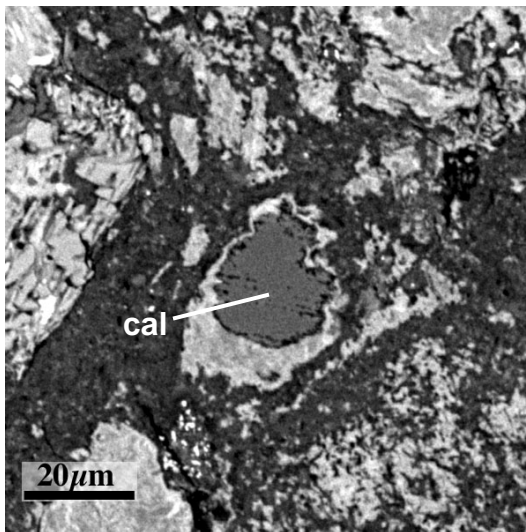
Type 2 (Clean) Carbonates



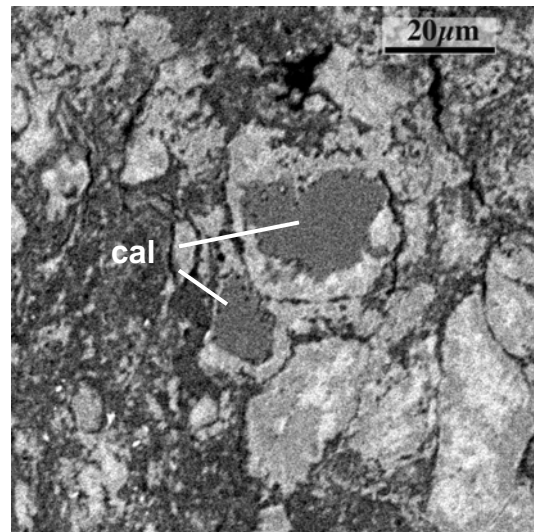
EET96019



Cold Bokkeveld

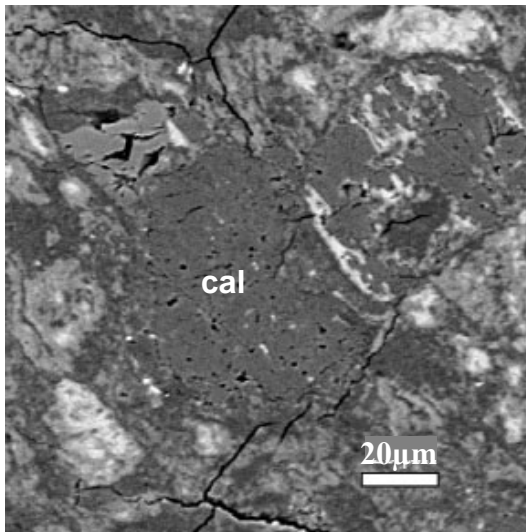


Cold Bokkeveld

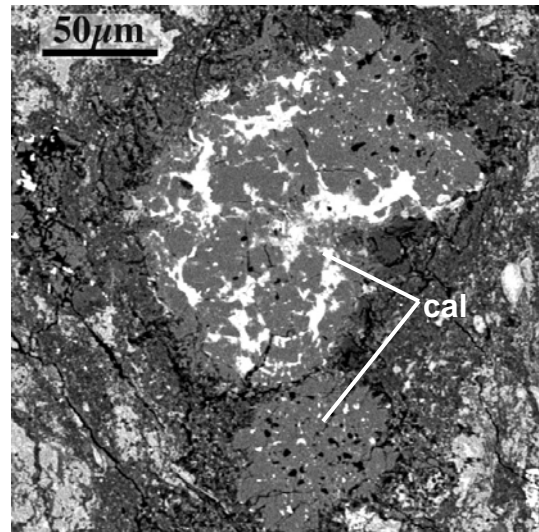


Murchison

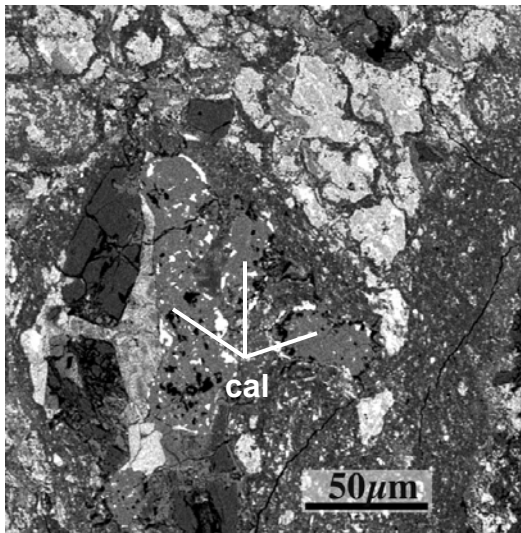
Type 3 (mottled) carbonates



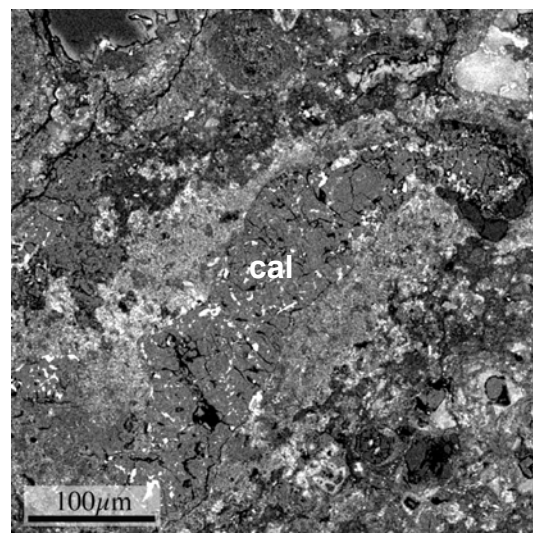
EET96019



Cold Bokkeveld



Cold Bokkeveld



Murchison

are noted to contain many unfilled fractures. The terrestrial weathering process redistributes meteoritic elements from the interiors to fractures and the surface as sulfates, carbonates, and salts (JULL *et al.*, 1988; RICIPUTI *et al.*, 1994; VELBEL *et al.*, 1991), and may also add extra meteorite components. Lee and Bland (2004) noted that terrestrial alteration products such as Fe-rich phyllosilicates fill intergranular pore-space as weathering proceeds. We will examine this question by focusing on the information gleaned from the petrographic characteristics of carbonates and also oxygen and carbon isotope analyses of the suite of paired EET samples.

In extraterrestrial and terrestrial environments, carbonate precipitation may be the likely result of silicate weathering reactions that consume acidity (CO<sub>2</sub>) and create the alkalinity required for carbonate formation. However, while terrestrial water which could react with the meteorite has oxygen isotopic compositions that fall along the TFL, meteoritic fluids would be <sup>17</sup>O-enriched relative to the TFL during parent body aqueous alteration processes. It is additionally possible that terrestrial fluids might evolve through interaction with meteoritic water. We suggest later in this study that this possibility can be evaluated with oxygen and carbon isotope data.

On the basis of petrographic observations, we suggest that the occurrences of carbonate minerals in the paired EET samples can be attributed to a combination of extraterrestrial and terrestrial processes. We interpret isolated, inclusion-free calcium carbonate grains in the EET samples (Fig. 5 a-d) to be the most likely candidates for an extraterrestrial origin, because of their similarities to subhedral inclusion-free grains in the CM2 falls (Fig. 9) studied by Benedix *et al.* (2003). In contrast, we interpret the fractures and veins filled with hydrated magnesium

carbonate in the paired EET samples to be the most likely candidates for carbonates of terrestrial origin. While Benedix *et al* (2003) and an earlier study by Bunch and Chang (1980) reported calcium carbonate veins for several CM2 chondrites falls (Muchison, Nogoya, and Cold Bokkeveld) and attributed to them an extraterrestrial origin, the vein carbonates in the EET samples that we studied (Fig. 5j-n) have a different composition (hydrated Mg carbonate along with minor calcium carbonate and dolomite). The most difficult carbonates in the EET samples to assess as extraterrestrial or terrestrial on the basis of textural grounds are the mottled calcium carbonate grains with irregular grain boundaries (Fig. 5e-i). These grains may be variants of the round calcite aggregates with included minerals observed in Nogoya by Benedix *et al.* (2003), but the authors did not report observing both subhedral calcite grains and subrounded calcite aggregates in the same meteorites. We suggest that the mottled appearance of these carbonate grains and the lower abundance of included anhydrous and sulfide mineral grains compared to the Nogoya observations of Benedix *et al.* (2003), may indicate that these EET carbonate grains were impacted by a higher degree of dissolution-reprecipitation and reaction, but we have not found evidence that allows us to distinguish whether these grains were produced by extraterrestrial processes, terrestrial processes, or some combination of the two. Our present data do not allow us to directly test this possibility, but future SIMS analyses may provide evidence that can be used to evaluate it.

#### 2.5.2.1 Evidence from Oxygen Isotopes

Bulk carbonate oxygen isotopic data for the EET paired finds are shown in Figure 6. Both Fig. 6-a and 6-b compare our findings with that of Benedix *et al.*

(2003) for CM2 falls. The oxygen isotopic composition of CM2 fall dolomite and calcite measured by Benedix *et al.* (2003) have similar  $\Delta^{17}\text{O}$ , but exhibit reversed fractionations ( $\delta^{18}\text{O}_{\text{dol}} < \delta^{18}\text{O}_{\text{cal}}$ ) than those expected from the same fluid (FRIEDMAN and O'NEIL, 1977). This same observation is made for the carbonate extracted from the paired EET samples, which may signify dolomite and calcite precipitated from unique or evolved solutions. The CM2 fall carbonates (calcium carbonate and dolomite, inclusive) form an array with a slope  $0.63 \pm 0.01$ , while EET paired finds form an array with a slope of  $0.48^{+0.03}_{-0.02}$ . These two lines are distinct and their intersection is interpreted to reflect the oxygen isotopic composition of the extraterrestrial carbonate component. Our bootstrap estimate (median) of the intersection occurs at  $\delta^{18}\text{O} = 29.6^{+1.4}_{-0.9} \text{‰}$  and  $\Delta^{17}\text{O} = -1.3^{+0.02}_{-0.1} \text{‰}$  (the central 2/3 of the resampled data is used because distributions have large asymmetric tails).

The intersection of the paired EET array with the TFL occurs at  $\delta^{18}\text{O} \approx +1\text{‰}$  with two thirds of the re-sampled data between  $+8\text{‰}$  and  $-16\text{‰}$ . One interpretation of this trend is that the array represents a mixing line between extraterrestrial carbonates and a terrestrial carbonate component. Isotopic exchange ( $\text{H}_2\text{O}$  with  $\text{HCO}_3^-$ ) associated with dissolution of extraterrestrial carbonate and the addition of terrestrial carbonate during recrystallization may explain the data array. At  $0^\circ\text{C}$ , the equilibrium isotopic difference between calcium carbonate and water ( $\alpha_{\text{CaCO}_3\text{-H}_2\text{O}} = 1.039$ ) is approximately  $38\text{‰}$  (ZHENG, 1999). Using our predicted intersection between the EET array and TFL, this would predict a  $\delta^{18}\text{O}$  value of the ice of  $-37^{+8}_{-16}$  given the large unsymmetrical uncertainty. Faure *et al.* (1988) measured  $\delta^{18}\text{O}$  ice at Elephant Moraine as  $-47.4 \pm 0.6\text{‰}$ , and this value is consistent with our interpretation

within error. It must be noted, however, that different regions of exposed ice at Elephant Moraine may have varied isotopic compositions, as ice is exposed at an angle. Because horizontal displacement encompasses temporal displacement and differing isotopic composition, the ice underlying this study's meteorites probably varied somewhat from the ice examined by Faure et al. (1988).

### 2.5.2.2 Evidence from Carbon Isotopes

#### *i. Carbon-14*

Radiocarbon, or  $^{14}\text{C}$ , has an atmospheric ratio of  $^{14}\text{C}/^{12}\text{C} = 1.17 \times 10^{-12}$  (JULL et al., 1989). Both  $^{12}\text{C}$  and  $^{13}\text{C}$  are stable isotopes while  $^{14}\text{C}$  decays with a half-life of 5730 years.  $^{14}\text{C}$  is continually created in Earth's atmosphere by interactions of nitrogen, carbon, and oxygen with cosmic rays. The most prevalent source of  $^{14}\text{C}$  is



where  ${}^1_1\text{H}$  is a proton and  ${}^1_0\text{n}$  is an impinging neutron (cosmic-ray particle) (FAURE, 1986). The carbon then can react with atmospheric oxygen or exchange with carbon in atmospheric  $\text{CO}_2$  or  $\text{CO}$  and are distributed worldwide.

Meteorites in space also may be bombarded by cosmic rays; however spallation of  $^{16}\text{O}$  to  $^{14}\text{C}$  is the most dominant mechanism of  $^{14}\text{C}$  formation (JULL et al., 1989; JULL et al., 1997). In this reaction, the incident cosmic ray removes 2 protons from the oxygen nucleus to form a  $^{14}\text{C}$  atom. Because silicates have more oxygen, by weight, more  $^{14}\text{C}$  will reside within silicate phases compared to carbonates. Saturated meteorite calcite has  $^{14}\text{C}$  concentrations of only 4.3% that of modern terrestrial atmosphere ( $\text{FMOD}^{14}\text{C} = 0.043$ ) (JULL et al., 1997).

The percentage of modern carbon-14 (F<sub>MOD</sub><sup>14</sup>C) in whole-rock and carbonate analyses have been used to determine the terrestrial age of Antarctic meteorites and to evaluate terrestrial contamination through the addition of atmospheric carbon (e.g., Goel and Kohman, (1962); Jull *et al.*, (1988); and Jull *et al.*, (1998)). Surface nuclear testing caused significant increases in the concentration of <sup>14</sup>C starting in 1950 and peaking in 1965 near a  $\Delta^{14}\text{C}_{\text{atm}}$  value of approximately 1000‰ or F<sub>MOD</sub><sup>14</sup>C  $\approx$  2, which represents a doubling of atmospheric <sup>14</sup>C (STUIVER and QUAY, 1981). Atmospheric <sup>14</sup>C levels have declined since 1965 as a result of the cessation of above ground nuclear testing and removal by ocean circulation. In addition, the input of fossil-fuels has diluted the radiogenic pool of CO<sub>2</sub> in the atmosphere (RUDDIMAN, 2001; STUIVER and QUAY, 1981). The carbon in EET carbonate is expected to have a F<sub>MOD</sub><sup>14</sup>C between 0 and 2. Sources with negligible F<sub>MOD</sub><sup>14</sup>C values include oxidized meteoritic organic matter (F<sub>MOD</sub><sup>14</sup>C  $\approx$  0), extraterrestrial carbonate (F<sub>MOD</sub><sup>14</sup>C < 0.043), and terrestrial non-atmospheric carbon (F<sub>MOD</sub><sup>14</sup>C  $\approx$  0) (JULL *et al.*, 1997). Organic matter F<sub>MOD</sub><sup>14</sup>C also should be near zero. Carbonates from <sup>14</sup>C-saturated meteorite falls contain minor <sup>14</sup>C from cosmic ray spallation of *in-situ* oxygen (JULL *et al.*, 1997), but the maximum radiocarbon expected in pure calcium carbonate would be  $3.2 \times 10^8$  atoms <sup>14</sup>C/g or an F<sub>MOD</sub><sup>14</sup>C of 0.043 (JULL *et al.*, 1995; JULL *et al.*, 1997). Some low <sup>14</sup>C terrestrial carbon (dead) could be incorporated from sedimentary rock and dust deposited at Elephant Moraine through dissolution and reprecipitation.

Sources with F<sub>MOD</sub><sup>14</sup>C greater than zero include atmospheric carbon and carbon produced by oxygen spallation reactions within extraterrestrial silicates. Jull

*et al.* (1988) noted surface-weathering products in a stony meteorite from an H5 chondrite that included very recent additions of carbonate with high  $^{14}\text{C}$  activity ( $1 < \text{FMOD}^{14}\text{C} < 2$ ). Silicate weathering reactions that consume atmospheric  $\text{CO}_2$  have the potential to produce alkalinity that would promote carbonate. In order for silicate-sourced  $^{14}\text{C}$  to be incorporated into terrestrial carbonate, the meteorite must have a young terrestrial age and significant silicate weathering, which would mobilize radiocarbon. In general, Elephant Moraine meteorites have a younger terrestrial age than many other meteorite-stranding surfaces (BENOIT *et al.*, 1994; HUSS, 1990). However, the meteorites are normally 40-50 ka in age, and possess surface exposure ages of  $< 12.5\text{ka}$  (BENOIT *et al.*, 1994; JULL *et al.*, 1989). By the time ice ablation had exposed the meteorites; multiple half-lives would have reduced  $^{14}\text{C}$  concentrations substantially. A more accurate portrait would be drawn if the meteorites were dated with multiple cosmogenic isotopes as achieved in Jull *et al.* (1989). Silicate-sourced  $^{14}\text{C}$  contamination was noted in Jull *et al.* (1997) during prolonged 4-5 day etching with 100%  $\text{H}_3\text{PO}_4$ . As stated above, silicates often have slightly higher cosmogenic  $^{14}\text{C}$  than carbonates (JULL *et al.*, 1997). However, contamination only becomes a problem during prolonged leaching of silicates that comprise the bulk of the meteorite (Calcite makes up on average only 0.44 wt%). The data shown in table 4 show no marked increase in  $\text{FMOD}^{14}\text{C}$  between the 3-hour and 18-hour extraction times, which indicate that the silicate  $^{14}\text{C}$  contamination was not significant in the EET analyses. Melt-water may also contribute dissolved terrestrial carbonate that would carry some of the  $\text{FMOD}^{14}\text{C}$  of its original source.

Table 4. C and O isotopic evaluation of paired Elephant Moraine CM2 meteorites. Columns denoted “WR” (whole-rock) were processed by laser fluorination and not acidification for bulk carbonate.

Sample/ Treatment	amount reacted (g)	CO <sub>2</sub> yield (μg/g)	Eq % <sup>a</sup> CaCO <sub>3</sub>	δ <sup>18</sup> O <sup>b</sup> (‰)	δ <sup>17</sup> O <sup>b</sup> (‰)	Δ <sup>17</sup> O <sup>b</sup> (‰)	δ <sup>13</sup> C <sup>c</sup> (‰)	FMOD <sup>14</sup> C	WR δ <sup>18</sup> O <sup>b</sup> (‰)	WR δ <sup>17</sup> O <sup>b</sup> (‰)	WR Δ <sup>17</sup> O <sup>b</sup> (‰)
<i>18 hrs 25°C acidification</i>											
EET96006	0.584	1470	0.333	24.87	11.90	-1.07	25.1	0.29	5.2	0.4	-2.35
EET96016	0.477	4140	0.941	27.78	13.17	-1.31	34.5	0.15	8.3	2.3	-2.01
EET96017	0.500	898	0.204	22.42	10.76	-0.94	12.9	0.33	5.8	0.5	-2.51
EET96018 <sup>d</sup>	0.401	3820	0.868	22.08	9.22	-2.31	48.9	0.08	6.0	0.7	-2.43
EET96019	0.550	1130	0.256	24.77	12.37	-0.55	8.4	0.45	5.7	0.4	-2.57
EET96029 <sup>d</sup>	0.449	263	0.0597	26.77	13.28	-0.67	36.0	0.09	2.4	-2.6	-3.82
<i>3 hrs 150°C acidification</i>											
EET96006	see above	769	0.175	22.55	10.65	-1.11	22.6	0.33	see above	see above	see above
EET96016		2750	0.624	28.00	13.35	-1.24	30.3	0.15			
EET96017		935	0.213	21.53	10.18	-1.06	12.7	0.33			
EET96018 <sup>d</sup>	see above	4730	1.07	21.00	8.66	-2.31	49.4	0.13	see above	see above	see above
EET96019		1110	0.251	22.79	11.00	-0.89	13.6	0.33			
EET96029 <sup>d</sup>		1080	0.246	23.54	11.79	-0.49	28.2	0.12			
<u>1 sigma</u>				0.03	0.07	0.03	0.1	0.02	0.4	0.2	0.05 <sup>e</sup>

<sup>a</sup>Equivalent amount of calcite by wt.% <sup>b</sup>Oxygen isotopic data referenced to SMOW, <sup>c</sup> δ<sup>13</sup>C referenced to VPDB, <sup>d</sup> not considered paired, <sup>e</sup> 0.3 on heterogeneity

Figure 7 compares  $\Delta^{17}\text{O}$  to  $\text{FMOD}^{14}\text{C}$  found within EET carbonate. The data form an array with a slope of  $0.40_{-0.07}^{+0.11}$  and a y intersection ( $\Delta^{17}\text{O} = 0\text{‰}$ ) at  $0.69_{-0.05}^{+0.13}\text{‰}$  (from  $\text{FMOD}^{14}\text{C} = a * \Delta^{17}\text{O} + b$ ). Where  $\text{FMOD}^{14}\text{C}$  equals zero,  $\Delta^{17}\text{O}$  is  $-1.64_{-0.12}^{+0.13}\text{‰}$ . As in section 2.5.2.1, we use a Monte-Carlo method to obtain the equations and uncertainties and report them for the central 2/3 of the data. Such a trend might be produced if different samples contained similarly high amounts of  $^{14}\text{C}$ , and underwent variable exchange of oxygen isotopes with the aqueous phase. Two arrays in the figure point to trends that would be expected in an open, or water-dominated, system with varying amounts of atmospheric  $^{14}\text{C}$ . In a water-dominated system, the oxygen isotopic composition of water is not influenced by interaction with meteorite minerals. The two arrays originate from points where  $^{14}\text{C}$  concentrations are assumed to be negligible and approach compositions where water-precipitated carbonate would be in equilibrium with atmospheric  $^{14}\text{C}$ . Another array shows hypothetical results in a closed, or rock-dominated, system. By definition the water in a rock dominated terrestrial weathering system will acquire some of its oxygen isotopic character from the minerals with which it reacts and the arrays no longer approach  $\Delta^{17}\text{O} = 0\text{‰}$ . Table 4 shows EET silicate minerals have negative  $\Delta^{17}\text{O}$  values, which follows observations made for other CM2 chondrites where  $\Delta^{17}\text{O}_{\text{carbonates}} > \Delta^{17}\text{O}_{\text{matrix}} > \Delta^{17}\text{O}_{\text{WR}} > \Delta^{17}\text{O}_{\text{anhydrous\_minerals}}$  (BENEDIX et al., 2003; CLAYTON and MAYEDA, 1999b). The data regression on this plot does not intersect the inferred initial  $\Delta^{17}\text{O}_{\text{carbonate}}$  value (Fig. 6-b), nor does it follow any prescribed array. This is interpreted to indicate that oxygen and carbon were not coupled during the formation of secondary carbonate. We suggest that this aspect of our data may

reflect a component of rock-dominated weathering. Carbonate grains in the matrix may have formed in a system where glacially-derived water exchanged its oxygen isotopes with silicate minerals during weathering and thus had a  $\Delta^{17}\text{O}$  that did not lie on the TFL. In this case, as in the water dominated case, the drive for formation of carbonate from atmospheric carbon sources is interpreted to be caused by alkalinity produced by silicate weathering reactions. This interpretation does not exclude the suggestion that water dominated weathering produced the carbonate filled veins in those meteorites.

*ii. Carbon-13*

Carbon-13, or  $^{13}\text{C}$ , data provides further information about carbon sources within EET carbonates. Figure 8 compares  $\delta^{13}\text{C}$  with both  $\Delta^{17}\text{O}$  and  $\text{FMOD}^{14}\text{C}$ . Fig. 8-a compares  $\Delta^{17}\text{O}$  to  $\delta^{13}\text{C}$  found within EET carbonate. The data form an array with a slope of  $-0.021^{+0.006}_{-0.005}$  and an intersection at  $-0.60^{+0.13}_{-0.17}$  (form  $\Delta^{17}\text{O} = a * \delta^{13}\text{C} + b$ , uncertainties are reported for the central 2/3 of the data). This line yields  $\delta^{13}\text{C}$  of  $-16^{+6}_{-21}$  ‰ when solved for  $\Delta^{17}\text{O} = 0$ ‰, a  $\delta^{13}\text{C}$  value that is more negative than carbonate precipitated from water in equilibrium with atmospheric carbon dioxide which suggests a more  $\delta^{13}\text{C}$  depleted second source of carbon. When this line is solved for  $\Delta^{17}\text{O} = -1.3$ ‰ (the EET/CMCL intersection),  $\delta^{13}\text{C} = 31 \pm 3$ ‰, which is a value that is  $^{13}\text{C}$ -depleted relative to carbonate from CM2 chondrite falls ( $44 \pm 13$  ‰) (GRADY et al., 1988). We suggest that this observation also indicates that some of the carbonates formed in a rock-dominated system and that aqueous fluids responsible for terrestrial weathering had undergone isotopic exchange with  $^{17}\text{O}$ -depleted silicates prior to precipitation of secondary carbonate. We do not favor alternative

explanations that require carbon isotope exchange without complementary oxygen isotope exchange, or preterrestrial oxygen and carbon isotope systematics of the EET carbonates to have differed in a fundamental way from the meteorite falls studied by Grady *et al.* (1988) and Benedix *et al.* (2003).

Figure 8-b compares FMOD<sup>14</sup>C to  $\delta^{13}\text{C}$  found within EET carbonate. The data form an array with a slope of  $-0.010^{+0.002}_{-0.001}$  and an intersection at  $0.48^{+0.03}_{-0.04}$  (from FMOD<sup>14</sup>C = a \*  $\delta^{13}\text{C}$  + b, uncertainties are reported for the central 2/3 of the data). When this equation is solved for the FMOD<sup>14</sup>C equals zero,  $\delta^{13}\text{C}$  is  $46 \pm 3\%$ , which also is consistent with the values reported by Grady *et al.* (1988). The intercept gives the average FMOD<sup>14</sup>C of this source if this line reflects simple addition of atmospheric carbon. However, because the average composition of atmospheric carbon is a value other than FMOD<sup>14</sup>C = 0.48, our regressed value of the intersection points to a second, non-atmospheric, source of carbonate carbon, which is consistent with inferences made on the basis of plot 4-a.

## 2.6 Conclusions

The purpose of this study was to construct a consistent picture of how CM2 meteorites and possibly other Antarctic meteorites are modified during interaction with the polar climate. We have shown that with paired meteorites we observe trends in carbonate oxygen and carbon isotopic space that weathering imparts upon these meteorites.

1. The  $\delta^{18}\text{O}$  vs.  $\delta^{17}\text{O}$  arrays reflect equilibration of terrestrial carbonate with Antarctic water.

2. Because FMOD<sup>14</sup>C implicates bomb carbon is within the carbonate, some percentage of terrestrial carbonate must have come from the atmosphere and was incorporated within the last 50 years.
3. Comparing  $\delta^{13}\text{C}$  with FMOD<sup>14</sup>C (and also  $\Delta^{17}\text{O}$ ) indicates a second  $\delta^{13}\text{C}$  depleted carbon source in terrestrial carbonate formation.
4. The  $\Delta^{17}\text{O}$  vs. FMOD<sup>14</sup>C trend is consistent with a component of the weathering occurring with water that evolved off of the TFL as a result of exchange with meteoritic silicates.

The whole-rock oxygen isotopic analysis revealed little difference in  $\Delta^{17}\text{O}$  that correlate with bulk-carbonate C and O isotopic results. Furthermore, measured bulk-carbonate isotopes did not correlate with carbonate yields (which differs from the results presented in Benedix *et al.* 2003). Even so, a reduction in absolute  $\Delta^{17}\text{O}$  corresponds with increasing FMOD<sup>14</sup>C throughout the meteorite carbonate set. This indicates a consistent carbonate-weathering picture. The inconsistency in whole-rock oxygen may primarily be due to heterogeneities within the meteorite body. Whole-rock analysis was of milligram quantities and is probably not representative of the entire meteorite.

One aspect that needs to be addressed is whether terrestrial carbonates are derived from glacially-dominated water or water that has exchanged with meteoritic water. A planned study to examine  $\delta^{13}\text{C}$  of matrix and vein carbonates using SIMS should show whether new carbonate formation is exclusively within the veins, or if new or reequilibrated material is interspersed throughout the meteorites. We were unsuccessful in constructing a comprehensive model that would explain our findings.

Without a working model, it is difficult to emplace criteria that will determine the extent of weathering, unless a paired set of meteorites is obtained. With a paired set, carbonate oxygen and carbon isotopic analysis can reveal much about the pre-terrestrial history of a meteorite. *In-situ* analyses may give added insights of the isotopic conditions that matrix and vein carbonates form and allow a working model to be created.

## **Chapter 3. Oxygen Isotope Heterogeneity in Calcite from CM2 Chondrites**

### 3.1 Introduction

Studies of CM2 carbonaceous chondrites have used the oxygen isotopic compositions of silicates, matrix, oxides, carbonates and sulfates to track the oxygen isotope evolution of water from which the minerals precipitated or interacted (AIRIEAU *et al.*, 2005; BENEDIX *et al.*, 2003; CLAYTON and MAYEDA, 1999a; CLAYTON and MAYEDA, 1984; ROWE *et al.*, 1994). Clayton and Mayeda (1984) described a model in which matrix oxygen isotope systematics in carbonaceous chondrites are explained by low temperature (<20°C) hydration reactions between two reservoirs: planetesimal water and anhydrous minerals. Benedix *et al.* (2003) documented the oxygen isotopic compositions of calcite in CM2 falls that defined an array with  $\delta^{17}\text{O} \approx 0.61 * \delta^{18}\text{O}$ , which was interpreted to have been produced during aqueous alteration of the parent asteroid. They demonstrated that a relationship exists between the extent of extra-terrestrial aqueous alteration and carbonate oxygen isotopic composition for CM2 meteorites.

In this paper secondary ionization mass spectrometry (SIMS) is used to examine carbonates in the same subset of paired Antarctic meteorites described in chapter 2. Specifically we use SIMS to further evaluate whether carbonates in a group of paired CM2 chondrites are terrestrial or extra-terrestrial and, if terrestrial, whether there is evidence that water oxygen exchanged with minerals within the meteorite matrix during the weathering process (rock-dominated water). SIMS evaluation of carbonate oxygen has been performed on other meteorites, including CM2 falls (Brearley *et al* 1999).

Here we report three *in-situ* oxygen isotopic analyses ( $^{16}\text{O}$ ,  $^{17}\text{O}$ , and  $^{18}\text{O}$ ) of CM2 calcite populations for 27 calcium carbonate grains. Additional work to analyze  $\delta^{13}\text{C}$  by SIMS is proposed as a future analytical target to further test the hypothesis.

## 3.2 Methods

### 3.2.1 Samples

The same four polished thick-sections of Antarctic meteorites EET96006, EET96016, EET96017, and EET96019 examined in Chapter 2 by EPMA were studied here by SIMS. These four samples were listed as paired in Lindstrom *et al.* (1998) and results in chapter 2 support this relationship.

### 3.2.2 SEM work

Sections were carbon-coated to a thickness of  $\sim 300\text{\AA}$  using standard thermal evaporation techniques and examined at the University of Maryland Center for Microscopy and Microanalysis with a JEOL JXA-8900 electron probe microanalyzer (EPMA) (15keV accelerated voltage, 1  $\mu\text{m}$  diameter beam) to locate and determine the chemical compositions of carbonate grains in these meteorites (Chapter 2, Table 1).

Prior to the SIMS analysis at the ASU GeoSIMS laboratory the carbon coating was removed. The removal process involved polishing away the carbon coating, followed by sonication (2x) in deionized water. After drying, the samples were gold-coated using a Hummer 6.2 Anatech sputter-coating unit (15 mA with 80-mTorr continual Argon gas flow). Additional imaging of the samples was performed prior to SIMS analysis on a JEOL JSM-IC845 Scanning Electron Microscope (SEM)

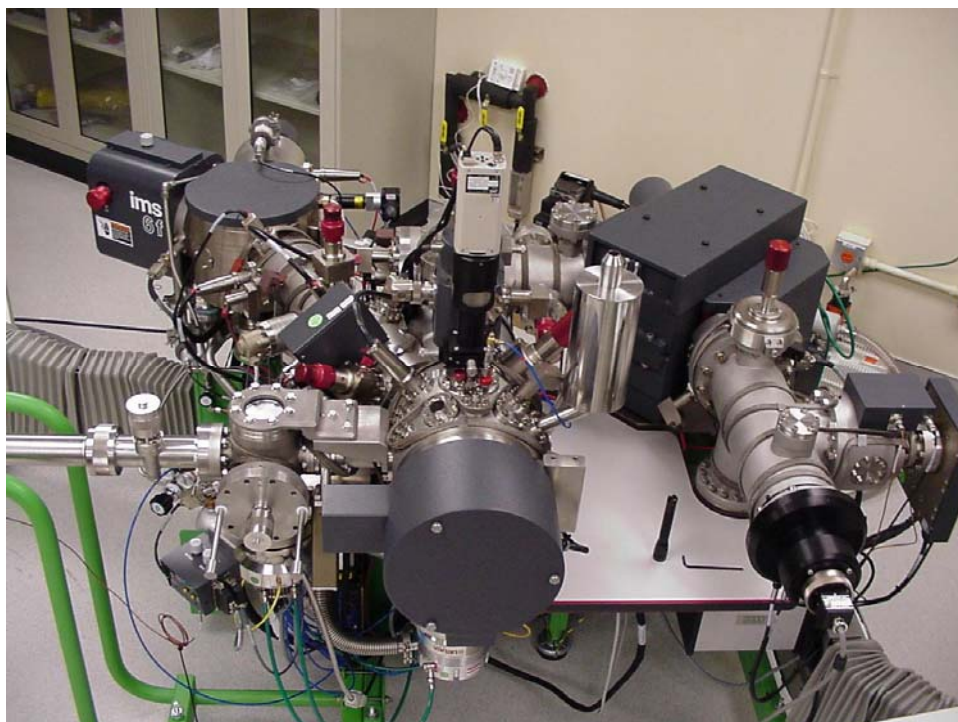
(15keV) located at ASU. Qualitative grain identification was performed with an IXRF energy dispersive X-ray analysis (EDX) system. Follow up SEM imaging was done after SIMS analysis to verify ion probe beam placement (Appendix 2).

### 3.2.3 SIMS

Oxygen isotopic analyses with the ASU CAMECA IMS 6F SIMS (Fig. 10) were done using a Cs<sup>+</sup> primary ion-beam (10 keV, ~25 $\mu$ m spot size in aperture illumination mode) with a normal incidence electron-flooding gun to provide charge neutralization. Secondary ions were measured with a mass resolving power (M/ $\Delta$ M) of ~6500, which well resolved <sup>17</sup>O from <sup>16</sup>OH. Counting times were 2 seconds for <sup>16</sup>O on a Faraday cup, 10 seconds for <sup>17</sup>O, and 4 seconds for <sup>18</sup>O on an electron multiplier (EM). Typical count rates of <sup>16</sup>O were 25-30 million counts per second. Background correction, which was negligible, was applied to all the three masses. EM dead time correction was applied to masses <sup>17</sup>O and <sup>18</sup>O and was 41 nanoseconds.

Instrumental Mass Fractionation (IMF) was determined to be 24.88‰ for  $\delta^{18}\text{O}$  and 12.44‰ for  $\delta^{17}\text{O}$  by analyzing a terrestrial calcite standard (Joplin calcite, with a  $\delta^{18}\text{O}$  value of 5.8‰). Uncertainties on individual analyses, taking into account the variation on repeated analyses of the standard, are 1.35 ‰ (1 $\sigma$ ) for  $\delta^{18}\text{O}$  and 1.4‰ (1 $\sigma$ ) for  $\delta^{17}\text{O}$ . Matrix effects are the cumulative IMF due to variances in sample chemical composition. Impurities measured by Wavelength Dispersive Spectroscopy (WDS) show that the studied calcite is relatively pure with <0.1 wt% Sr, <0.1 wt% Mn, and <1 wt% Mg, <2 wt% Fe (Chapter 2, Table 1). Because the analyzed calcite is very similar to the composition of the standard we do not use additional matrix-effect corrections.

**Figure 10.** Photograph of SIMS at the Arizona State University GEOSIMS laboratory. Photograph courtesy of Paul Niles.



### 3.3 Results

We report the  $\delta^{18}\text{O}$ ,  $\delta^{17}\text{O}$ , and  $\Delta^{17}\text{O}$  of calcite on all four samples in Table 5. The analyses in Table 5 are grouped on the basis of the carbonate morphology into two basic types of calcite, “mottled” and “clean”. Also included are two vein calcites (one of which was discarded due to beam placement). The rarity of vein calcite of adequate size for SIMS analysis limited us to two acceptable crystals. Because tohilinite grains are often adjacent to or surround calcite, one tohilinite grain was also analyzed exclusively (EET96019\_bx16 spot d). Although we undertook no additional IMF calibration for this grain, measured oxygen isotopic composition is indistinguishable from the calcite that it surrounded (EET96019\_bx16 spot c).

A total of 21 distinct “clean” calcites and 4 “mottled” calcites were analyzed, some repeatedly. The two populations of calcite have two distinct isotopic compositions. “Clean” calcite has a  $\delta^{18}\text{O}$  of  $33.6 \pm 2.3\text{‰}$ , whereas “mottled” calcite has  $\delta^{18}\text{O}$  values of  $19.4 \pm 1.5\text{‰}$ . Clean and mottled calcites also have different  $\delta^{17}\text{O}$  and  $\Delta^{17}\text{O}$  values. While these values fall near the ends of the Benedix et al. (2003) array, they fall on either side of the EET bulk-carbonate array from samples in Chapter 2. If we consider the average values (reporting 2X standard error or 2SE) of clean and mottled carbonate, we obtain  $\delta^{18}\text{O} = 33.7 \pm 0.8$  (2SE) and  $19.4 \pm 1.0$  (2SE) and  $\Delta^{17}\text{O} = -0.8 \pm 0.4\text{‰}$  (2SE) and  $-2.0 \pm 0.6\text{‰}$  (2SE). The observed differences between different carbonate grains are not unexpected, because we have progressed from a bulk-rock to an *in situ* technique.

Table 5. Oxygen isotopic compositions within select EET carbonate grains. Notes show where some incorporation of surrounding material occurred, but seems to have little effect upon results.

FILE/comment	type <sup>1</sup>	$\delta^{18}\text{O}$ (‰)	1 $\sigma$ (‰)	$\delta^{17}\text{O}$ (‰)	1 $\sigma$ (‰)	$\Delta^{17}\text{O}$ (‰)	1 $\sigma$ (‰)	notes <sup>2</sup>
"clean" calcite								
EET96006_bx2a1	C	35.5	1.6	16.8	1.1	-1.6	0.9	
EET96006_bx2a2	C	36.1	1.6	17.6	1.2	-1.1	1.0	
EET96006_bx4a	C	34.3	1.6	18.0	1.2	0.1	1.0	
EET96006_bx11a	C	29.8	1.6	14.1	1.1	-1.4	0.9	
EET96006_bx11b	C	30.0	1.6	14.3	1.2	-1.3	1.0	
EET96006_bx2c	C	33.8	1.5	16.1	1.3	-1.5	1.1	
EET96006_bx2a3	C	35.1	1.4	16.7	1.6	-1.6	1.2	
EET96019_bx16a	C	28.8	1.5	13.9	1.7	-1.0	1.4	
EET96019_bx16b	C	31.7	1.5	15.3	1.6	-1.2	1.2	~1/4 contamination
EET96019_bx16c	C	33.6	1.4	16.6	1.6	-0.9	1.2	<1/4 contamination
EET96019_bx16e	C	33.2	1.4	17.2	1.5	-0.1	1.1	
EET96019_bx9b	C	34.1	1.5	15.7	1.5	-2.0	1.2	
EET96019_bx9c	C	36.3	1.5	18.3	1.6	-0.5	1.2	<1/4 contamination
EET96019_bx18b	C	35.6	1.5	17.4	1.6	-1.1	1.2	
EET96019_bx19a	C	31.4	1.5	14.7	1.6	-1.6	1.2	
EET96019_bx20a	C	34.6	1.5	17.2	1.6	-0.8	1.2	
EET96016_bx18a	C	36.7	1.4	20.9	1.5	1.9	1.1	~1/4 contamination
EET96016_bx12b	C	33.9	1.4	17.1	1.7	-0.5	1.3	
EET96016_bx15a	C	31.6	1.4	17.2	1.6	0.8	1.2	<1/4 contamination
EET96016_bx15b	C	32.9	1.5	15.3	1.5	-1.7	1.1	
EET96017_bx15a	C	33.0	1.4	16.0	1.6	-1.2	1.2	~1/4 contamination
EET96017_bx16a	C	34.2	1.5	17.3	1.6	-0.5	1.3	~1/4 contamination
EET96017_bx4a	C	37.8	1.5	19.6	1.6	0.0	1.2	
"mottled" calcite								
EET96006_bx3a1	M	18.7	1.6	6.1	1.1	-3.6	0.9	
EET96006_bx3a2	M	19.7	1.6	7.4	1.3	-2.8	1.1	
EET96019_bx9a	M	21.1	1.4	9.2	1.5	-1.8	1.1	
EET96019_bx18a1	M	20.8	1.4	10.1	1.6	-0.7	1.2	
EET96019_bx18a2	M	20.6	1.4	8.9	1.7	-1.8	1.3	
EET96016_bx9a1	M	19.6	1.5	8.3	1.5	-1.9	1.1	
EET96016_bx9a2	M	16.8	1.4	6.9	1.5	-1.8	1.0	
EET96016_bx9a3	M	18.1	1.5	8.0	1.7	-1.5	1.4	
other calcite								
EET96019_bx16d	T	30.9	1.5	15.7	1.6	-0.4	1.2	
EET96016_bx20a	V	-5.3	1.4	-3.3	1.5	-0.5	1.1	

<sup>1</sup> types include C (clean), M (mottled), V (vein), and T (tochilinite, not a calcite)

<sup>2</sup> Visual inspections reveal some contamination with surrounding material (usually tochilinite) on some grains.

### 3.4 Discussion

#### 3.4.1 Comparison of SIMS results with bulk-carbonate data

With the preceding results we can make the following general statements. The two matrix calcites, clean and mottled, represent different generations of calcite formation. The slopes produced by the two populations within this study represent only the largest calcite in the section due to SIMS spot diameter and therefore may not represent all matrix calcite populations.

Figure 11 presents the SIMS analyses of the four Elephant Moraine meteorites. The isotopic results of the two populations are related to calcite type. The  $\delta^{18}\text{O}$  of the two carbonate types, regardless of level of weathering, remain consistent regardless of which sample is analyzed. The EET/CMCL bulk-carbonate array intersection reported in Chapter 2 is inferred to be an average of the two carbonate populations.

A comparison of the results of this study ( $\delta^{18}\text{O}$  vs.  $\Delta^{17}\text{O}$ ) with the bulk-carbonate results indicates that the bulk-carbonate data lie between the mottled and clean carbonate populations (Figure 12). This may indicate that values reported in Table 4 are averages of the two dominant calcite populations, but this interpretation would be inconsistent with the trend of the EET array. Although the *in-situ* SIMS analyses have a positive slope, the bulk-carbonate data possess a trend with a negative slope that approaches the TFL at near  $\delta^{18}\text{O} \sim 0\text{‰}$  and  $\Delta^{17}\text{O} \sim 0\text{‰}$ . Taken together, the data are interpreted to be the mixing of three reservoirs: clean carbonate, mottled carbonate, and terrestrial carbonate.

**Figure 11.** Three isotope plot ( $\delta^{17}\text{O}$  vs.  $\delta^{18}\text{O}$ ) relative to Standard Mean Ocean Water (SMOW) of *in-situ* matrix carbonates. “Clean” and “mottled” carbonates are distinct. “TFL” refers to the Terrestrial Fractionation Line, derived by terrestrial silicates and waters (MILLER, 2002).

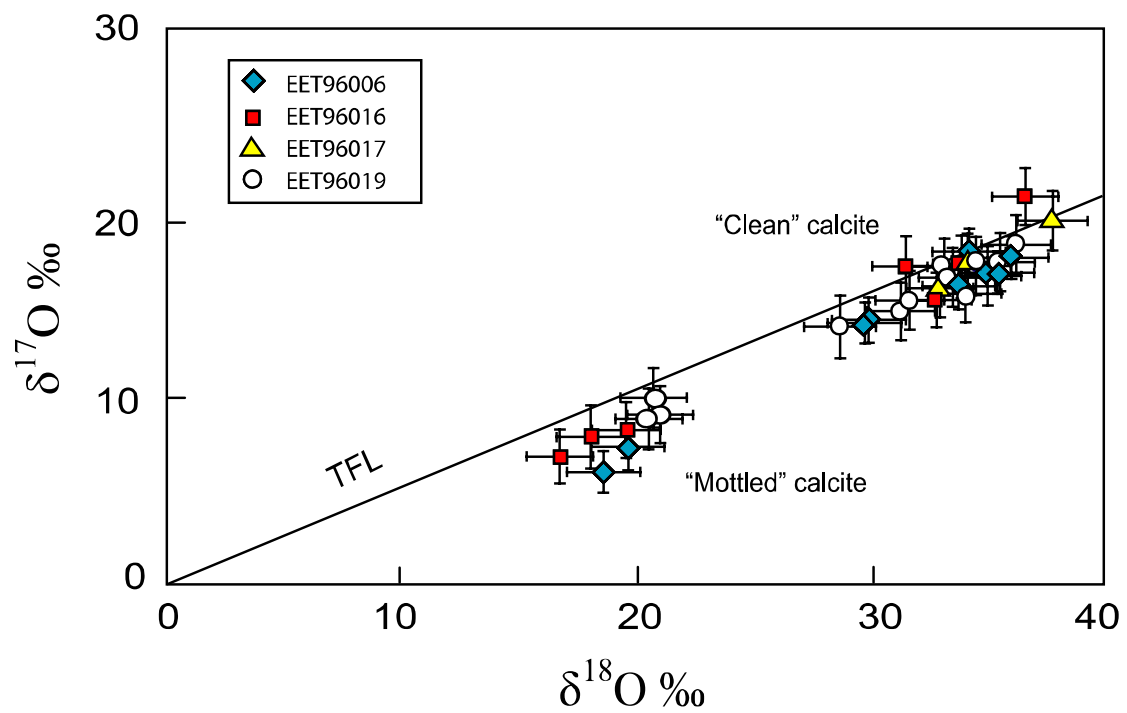
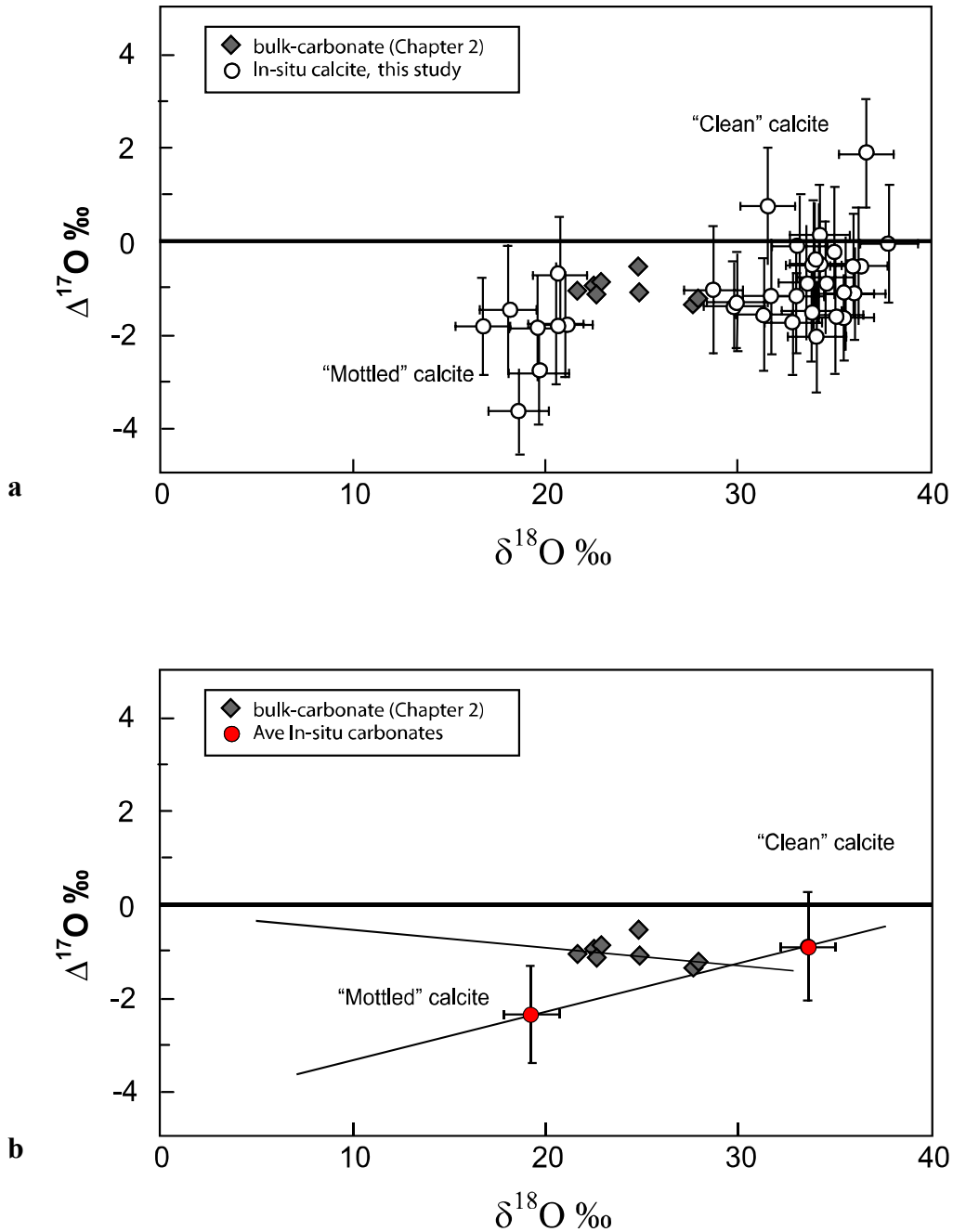


Figure 11

**Figure 12**

$\Delta^{17}\text{O}$  vs.  $\delta^{18}\text{O}$  for *in-situ* carbonates from this study and bulk carbonate data from Chapter 2. Bulk carbonate  $\Delta^{17}\text{O}$  values appear elevated and indicate a terrestrial component in the bulk data not found in individual matrix carbonates. Fig. 12-a shows the individual data points and Fig. 12-b shows averages of SIMS data by type.



The  $\delta^{18}\text{O}$  and  $\Delta^{17}\text{O}$  SIMS data of this study demonstrate that the CM2 fall bulk carbonate of Benedix *et al.* (2003) could be represented by mixtures of mottled and clean calcite (Figure 13). In this figure, the CM2 fall data appear to be directly related in trend and scope with EET carbonates examined by SIMS. It is possible that the Benedix *et al.* (2003) array could be explained by heterogeneities within calcite types and the amount of calcite present within a sample. If we were to connect the average values of clean and mottled carbonates (SIMS) in a  $\delta^{18}\text{O}$  vs.  $\delta^{17}\text{O}$  plot, we would have a line with a slope of 0.60; The CM2 fall array has a slope of  $0.63 \pm 0.01$  (see pg. 37). The CM2 falls data extend further than the EET bulk-carbonate into the fields of both mottled and clean calcites. Because these meteorites were falls with minimal terrestrial processing and the similarities in oxygen isotopes with the two carbonate populations, the Benedix *et al.* (2003) data support two of the three reservoirs that are involved with the EET bulk-carbonate trend. As expected by the pristine condition CM2 falls exhibit, terrestrial carbonate is not present.

### 3.4.2 Observations and Model

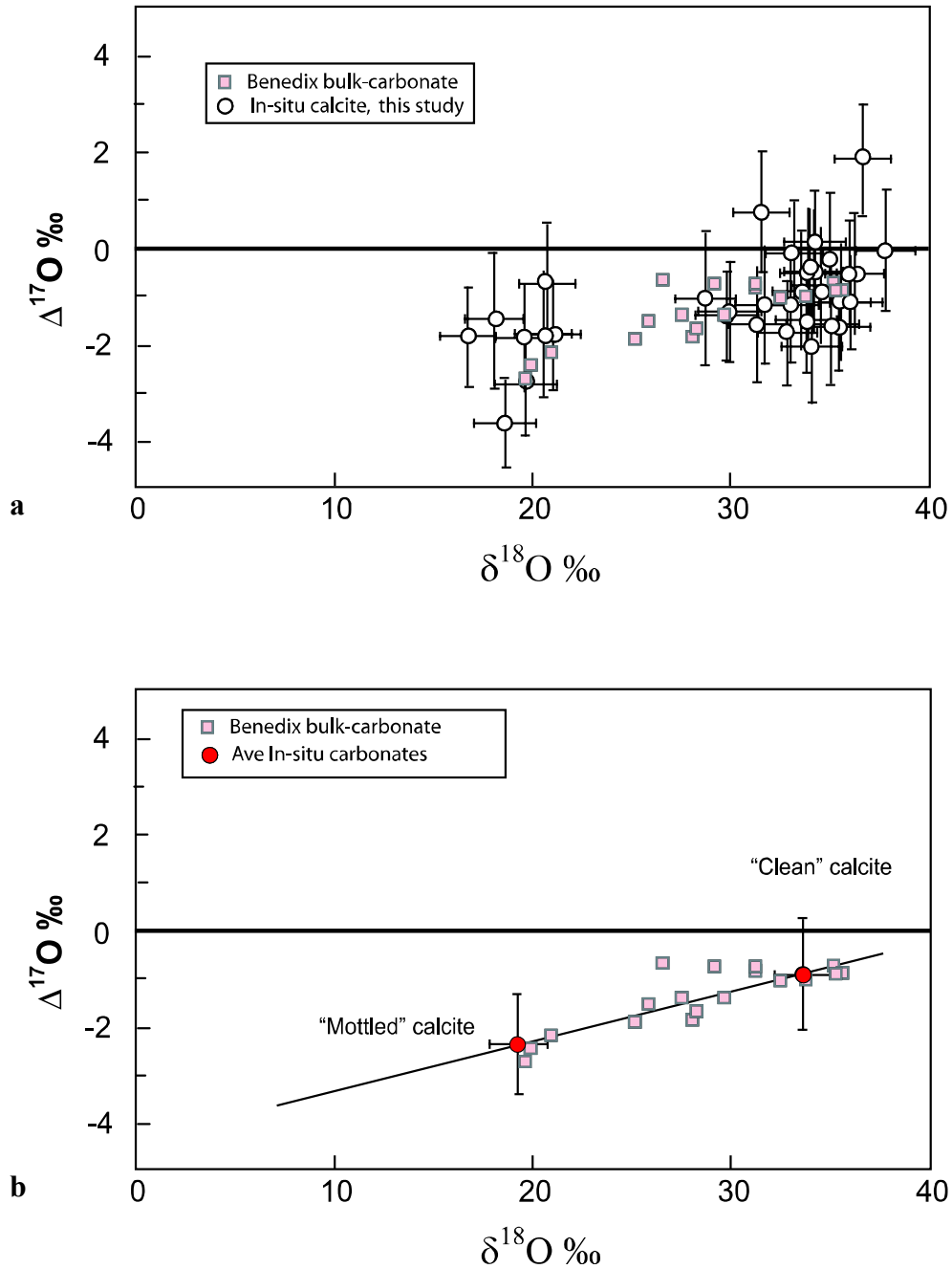
The population of upper  $\delta^{18}\text{O}$  calcite, or “clean” calcite, as discussed above, is ubiquitous among CM2 meteorites and is thus probably the oldest calcite analyzed in this study. Brearley *et al.* (1999b) studied Murchison, the least aqueously altered CM2 fall, carbonates *in-situ* by SIMS and found that they varied from 27.4 to 37.2 ‰ ( $\delta^{18}\text{O}$ ), which is similar to the data of this study ( $33.6 \pm 2.3\%$ ).

While “clean” carbonates are ubiquitous to the CM2 meteorite population, another type of carbonate, “mottled” carbonates have only been noted in one of the most aqueously altered CM2 meteorite, Cold Bokkeveld (Benedix, personal

communication). This suggests “clean” carbonates formed first. Mottled calcite, on the other hand, was not noted within the listing of calcite types discussed in Benedix *et al.* (2003). The history of this variety of calcite is unclear. The oxygen isotopic composition of the mottled calcite suggests that it formed from more  $^{17}\text{O}$ -depleted water than the water from which the clean calcite formed. This may have occurred as part of the continued extraterrestrial alteration process, or it may have occurred during terrestrial weathering, provided there was a process that could produce water with appropriate  $^{17}\text{O}$ -depleted compositions. Some calcite in the CM2 meteorite Nogoya may be related to mottled calcite. This calcite is amorphous and includes phenocrysts of olivine and pyroxene within the grains (BENEDIX *et al.*, 2003). A few calcites in Cold Bokkeveld (the most altered sample examined by Benedix *et al.* 2003) resemble mottled calcites (Benedix, personal communication). Further study is necessary of to determine if mottled calcite occurs in other CM2 falls.

One SIMS analysis exists of a vein calcite and we were unsuccessful in our attempts to analyze Mg-carbonates because ion count rates were very low compared to our standard magnesite, possibly due to their hydration state or structure. The single vein calcite that was analyzed gave values consistent with predictions made in Chapter 2 (Fig. 6-b) at a  $\delta^{18}\text{O} = -5.34 \pm 1.45 \text{ ‰}$ ,  $\delta^{17}\text{O} = -3.29 \pm 1.49 \text{ ‰}$  and a  $\Delta^{17}\text{O} = 1.07 \pm 1.07 \text{ ‰}$ , and is interpreted to represent a terrestrial carbonate endmember in the EET meteoritic carbonate population.

**Figure 13.**  $\Delta^{17}\text{O}$  vs.  $\delta^{18}\text{O}$  data for *in-situ* carbonates (this study) and that of Benedix *et al.* 2003 for CM2 meteorite falls. The CM2 fall data overlap the two calcite populations directly, with no terrestrial component evident. Fig. 13-a shows the individual data points and Fig. 13-b shows averages of SIMS data by type.



A conceptual model to illustrate water isotopic evolution that describes the possible endmember cases for extraterrestrial and terrestrial aqueous alteration is presented in Figure 14. Fig. 14-a combines the model of Clayton and Mayeda (1999a) for chondrite matrix formation with that of Benedix *et al.* (2003) for meteorite carbonate formation. Clayton and Mayeda (1999a) initially proposed that matrix mineral oxygen isotopic signatures are a result of the mixing of two reservoirs: oxygen in anhydrous silicate phases and oxygen in planetesimal or nebular water (Fig. 14-a). As the oxygen isotopic signature of planetesimal water evolved toward the silicate signature, carbonates crystallizing in equilibrium with the water preserve the water's evolving oxygen isotopic signature at the time of formation (Fig. 13). The SIMS data are consistent with "clean" calcite having oxygen isotopic signatures that preserve the crystallization of the calcite in equilibrium with such an evolving fluid.

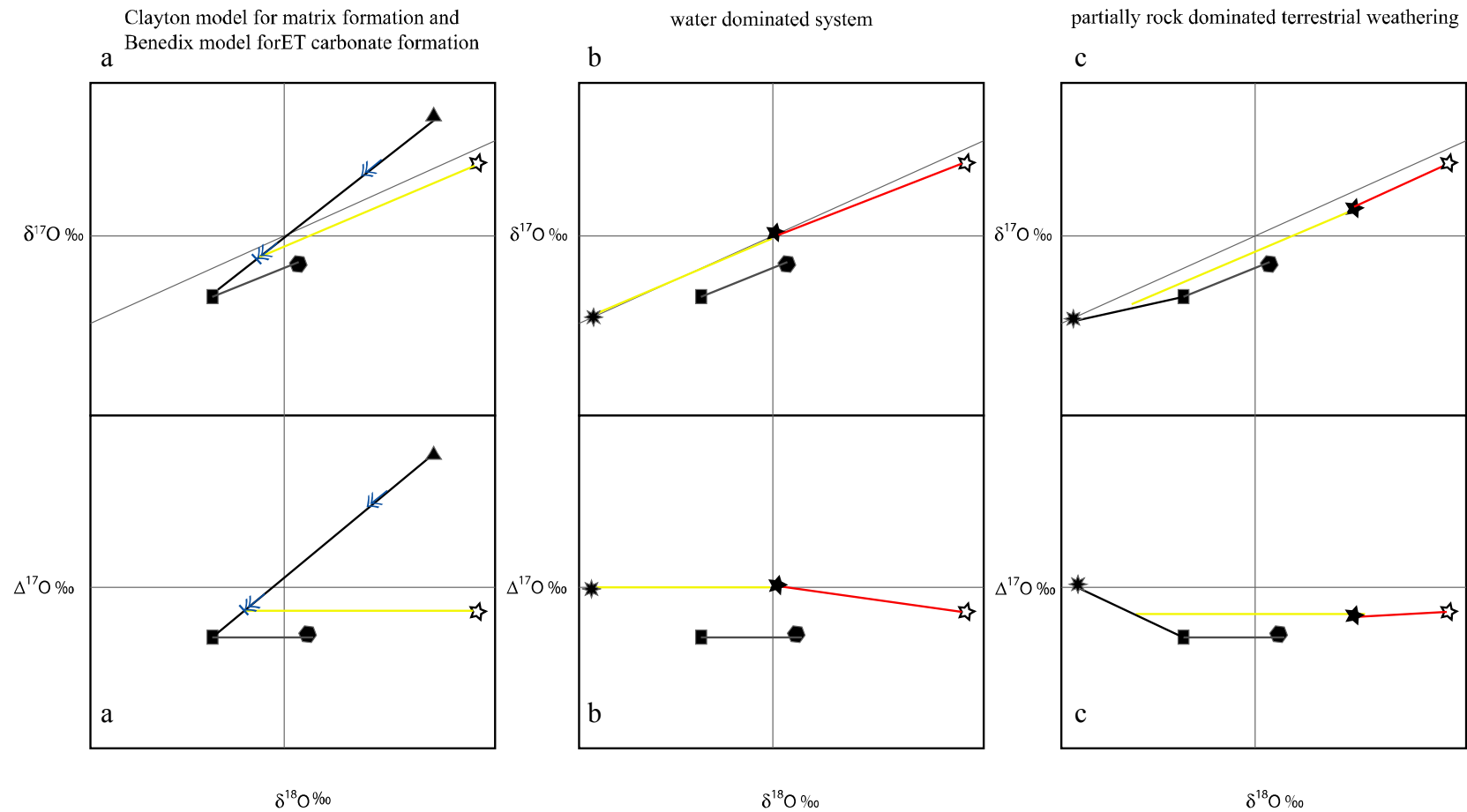
Terrestrial calcite in a water-dominated system would form in equilibrium with ice and have  $\delta^{18}\text{O}$ ,  $\delta^{17}\text{O}$ , and  $\Delta^{17}\text{O}$  near 0‰. Terrestrial water-dominated conditions should be realized in meteorites where glacial water can flow freely through their interiors. Meteorite falls are normally highly fractured (and the EET parent seems not to have been an exception), providing openings for water to wick from the summer water saturated base to the top where it evaporates. Surficial evaporate minerals on the majority of carbonaceous chondrites show that water transport through meteorites is common upon the ice sheet (BLAND *et al.*, 2000; BLAND *et al.*, 1998; JULL *et al.*, 1988; LEE and BLAND, 2004). Velbel (1988) noted carbonaceous chondrites make up only 2% of the Antarctic meteorite population, but

encompass 1/5 of those with surface evaporites. A representation of terrestrial carbonate formation is shown in Fig. 14-b.

Water that has exchanged extensively with meteorite silicates (rock dominated) may also be found within meteorites and a conceptual model of the oxygen isotope compositions is illustrated in Figure 14-c. Terrestrial water may travel through tiny ( $\sim 10 \mu\text{m}$  in diameter) pores and fractures, encountering a large meteoritic rock surface area in which to react. Water that makes it into the porous matrix may stagnate and become even more rock dominated. Oxygen isotopic compositions of mottled carbonate may have formed either in such a terrestrial system, or they may reflect an extraterrestrial rock-dominated carbonate formation event that occurred from an evolved ( $^{16}\text{O}$ -rich) fluid after formation of clean carbonates. Unfortunately, the data do not resolve which trends are followed as terrestrial weathering proceeds. With only oxygen isotopic data, we cannot be certain whether mottled carbonates are primarily extraterrestrial, primarily terrestrial, or both. Formation of mottled carbonates may be modeled, however (Fig. 14-c). This process also could have occurred upon the CM2 meteorite parent body long before impact.

**Figure 14.** Illustration of a model of carbonate evolution within EET meteorites.

- a. Clayton and Mayeda (1999a) model of planetesimal water evolution as it exchanges with silicates combined with the model of Benedix *et al.* (2003) showing extraterrestrial carbonate precipitating from this fluid in isotopic equilibrium. This scenario may represent conditions “clean” calcites formed.
- b. Carbonate formation in a terrestrially-dominated system, where carbonate precipitates in equilibrium with terrestrial glacial water.
- c. Formation of mottled calcite. The line connecting water in equilibrium with the meteorite to terrestrial water represents the composition of terrestrial water in various stages of rock domination. These carbonates have more negative  $\Delta^{17}\text{O}$  values than clean calcite.



- ▲ extraterrestrial water
- \* glacial water
- water in equilibrium with meteorite
- meteorite whole rock
- ☆ extraterrestrial carbonate (formed from Evolved ET water)
- ★ Terrestrial carbonate formed in contact with water (evolved water in case of rock dominated system)

Figure 14

### 3.5 Conclusions

SIMS analyses of oxygen isotopes reveals new information on the origins of the three dominant calcite types in the studied paired EET meteorites. This data show that the isotopic composition of “clean” and “mottled” carbonate bracket extremes within the Benedix *et al.* (2003) array. Bulk carbonate, studied in Chapter 2, also fall between the two carbonates in  $\delta^{18}\text{O}$ -space; however, the measured  $\delta^{17}\text{O}$  behave differently. We present a model that shows three mechanisms for carbonate formation. The first encompasses the mechanism described in Benedix *et al.* (2003), in which carbonate formation marks large-scale water oxygen isotope evolution as original nebular water exchanges oxygen with meteoritic silicates. The second explains the trend discussed in Chapter 2 where water, which has a dominantly terrestrial oxygen isotopic signature, hosts the carbonate ions and precipitates carbonates predominantly in fractures. The last mechanism shows that the oxygen isotopic signature of mottled calcite can be explained by either rock-dominated fluid within the parent body or terrestrial water becoming rock dominated producing calcite within the meteorite. The third hypothesis can be tested by further SIMS carbonate *in-situ* carbon isotopic analysis. We would expect extraterrestrial carbonates to have  $\delta^{13}\text{C}$  values near the CM2 fall range reported by Grady *et al.* (1988) of  $+44 \pm 13$  ‰ and terrestrial carbonate to have negative  $\delta^{13}\text{C}$  values as shown in Fig. 8 a and b.

## **Chapter 4. Work Summary**

In this study we examined a set of paired CM2 meteorite finds from Elephant Moraine, Antarctica. Carbonates were examined with an electron microprobe visually and with WDS beam elemental analysis. Bulk carbonate isotopic analysis was performed by converting carbonates to CO<sub>2</sub>. We also examined carbonates *in-situ* with a SIMS. The purpose was to discover where and how carbonates in Antarctic CM2 finds formed.

SEM imaging of the paired EET suite of meteorites identified four carbonate morphologies. Type 1 carbonate may be an isolated case and not be important to the meteorite set as a whole. Type 2 carbonates, “clean” carbonate, resemble carbonates found in most CM2 meteorites, and may be ubiquitous to CM2 meteorites. Type 3, “mottled” carbonate, appear throughout the EET sample suite and also may appear in a CM2 meteorite that experienced extensive aqueous alteration (Cold Bokkeveld). Type 4 carbonates, the vein carbonates, were composed mostly of Mg-carbonate fracture-fill. Calcite and isolated dolomite also was found within veins.

A multi-isotope approach ( $\delta^{18}\text{O}$ ,  $\delta^{17}\text{O}$ ,  $\Delta^{17}\text{O}$ ,  $\delta^{13}\text{C}$ , and FMOD<sup>14</sup>C) for discriminating the origins of the types of calcite was attempted using bulk-carbonate techniques. All data formed trends, but not all trends agreed with the other. Through oxygen isotopes, we determined an extraterrestrial carbonate component ( $\delta^{18}\text{O} \approx 29.8$  ‰ and  $\Delta^{17}\text{O} \approx -1.25$  ‰) and a terrestrial component that was consistent with precipitation from melted glacial water ( $\delta^{18}\text{O} \approx 1$ ,  $\delta^{17}\text{O} \approx 0$ ). Carbon-14 analysis showed that a recent atmospheric carbon component evident; while  $\delta^{13}\text{C}$  measurements showed a depleted dead carbon component is influencing terrestrial carbonate composition.

*In-situ* SIMS oxygen isotope analysis resolved differences in two matrix carbonates (clean and mottled) that bracket both the EET bulk-carbonate data and the  $\delta^{18}\text{O}$  data in CM2 Falls. Clean carbonate appears to be extraterrestrial and the origin of mottled carbonate could be either extraterrestrial or terrestrial. No carbonate (except, possibly, the lone vein-carbonate data point) examined with SIMS proved to definitely be the terrestrial carbonate component.

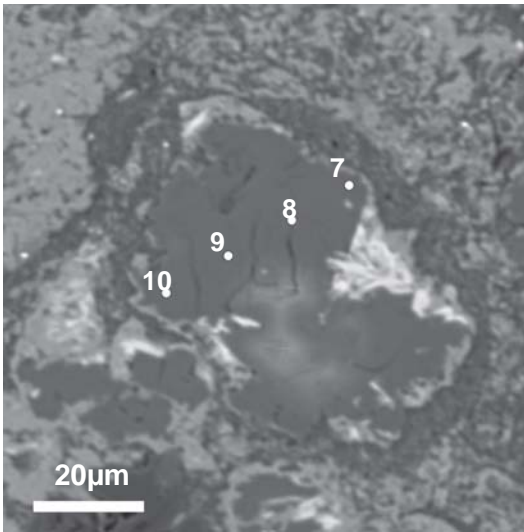
We have constructed a representation that evaluates three modes of carbonate precipitation within the EET meteorite suite. Clean calcite is interpreted to have preserved isotope information about the planetesimal water as it evolved. Terrestrial carbonate formed in an open, water-dominated environment preserve information from differing sources: glacial water, atmospheric  $\text{CO}_2$ , and another depleted dead carbon source. Mottled carbonate was formed in conditions, either terrestrial or extraterrestrial, where significant exchange with meteorite silicates completely dominates the oxygen isotope setting.

The goal to determine general trends inherent Antarctic meteorite carbonate C and O isotope systems was only partially successful. We would require *in-situ* analysis of extraterrestrial carbonates to determine if three carbonate types also dominate carbon isotopes. With this information, we can then constrain C and O terrestrial inputs into terrestrial carbonate formation. Determining, for instance, whether the oxidation of meteorite organic matter could be a source for the  $\delta^{13}\text{C}$  depleted dead carbon component, may then be possible.

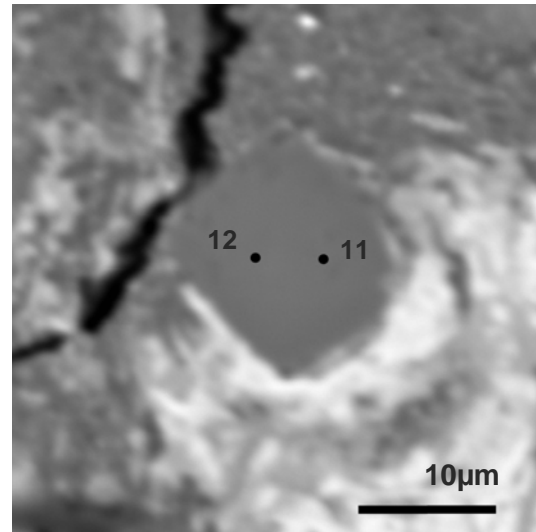
## Appendix 1

**Figure 15.** Spot locations of EPMA WDS elemental analyses. The methods employed are explained in the chapter 2 methods section. Data from spots displayed in Table 1.

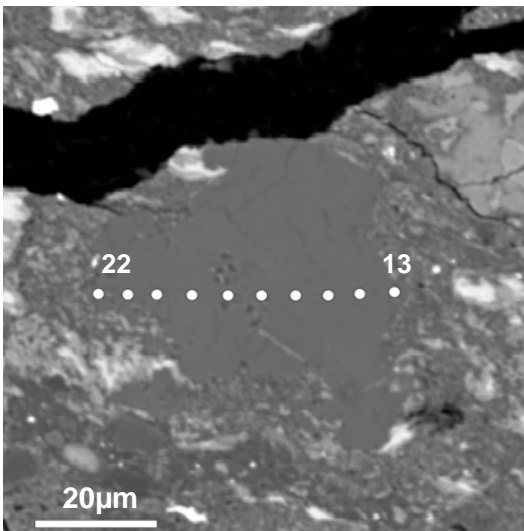
EET96019



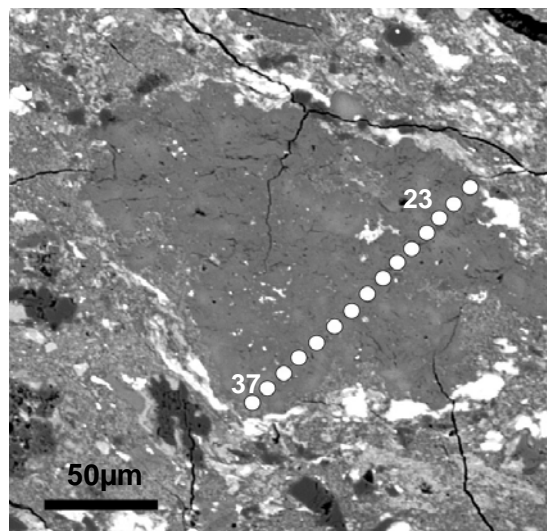
EET96019



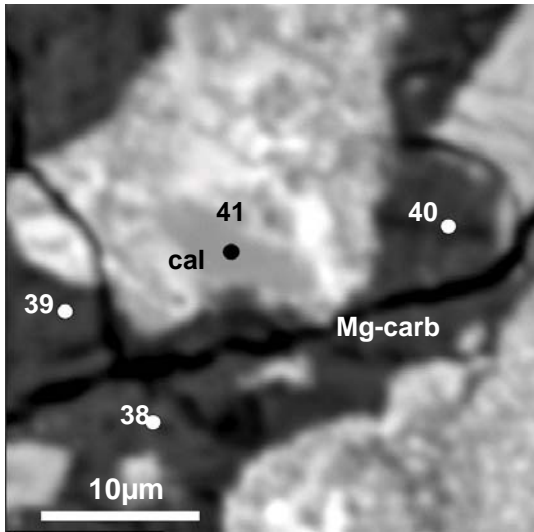
EET96019



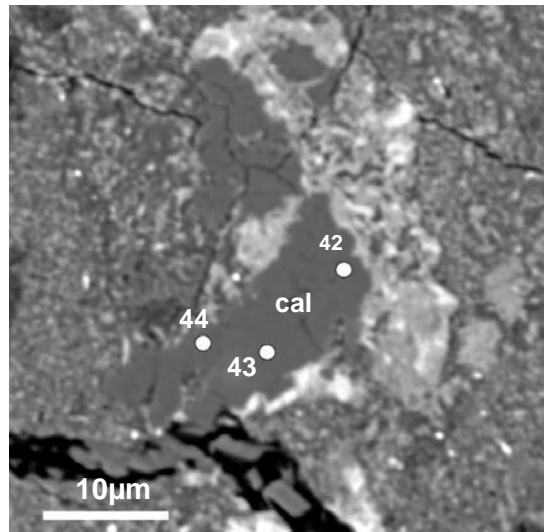
EET96016



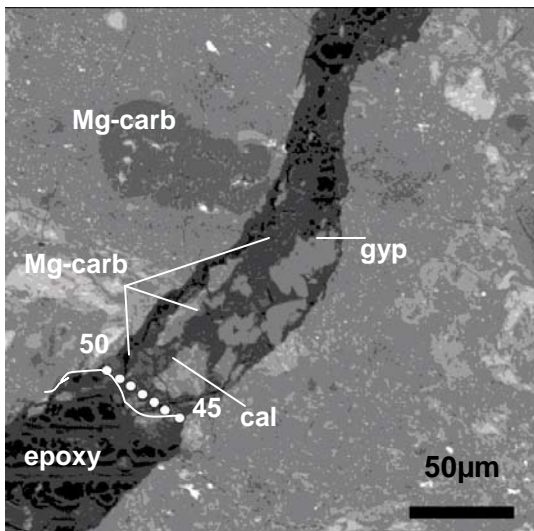
EET96006



EET96006



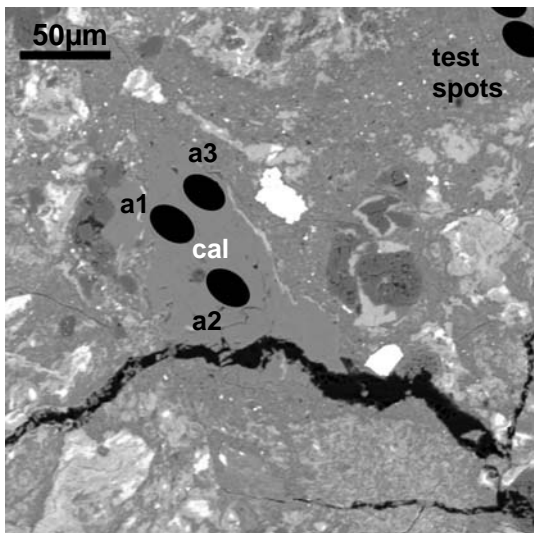
EET96006



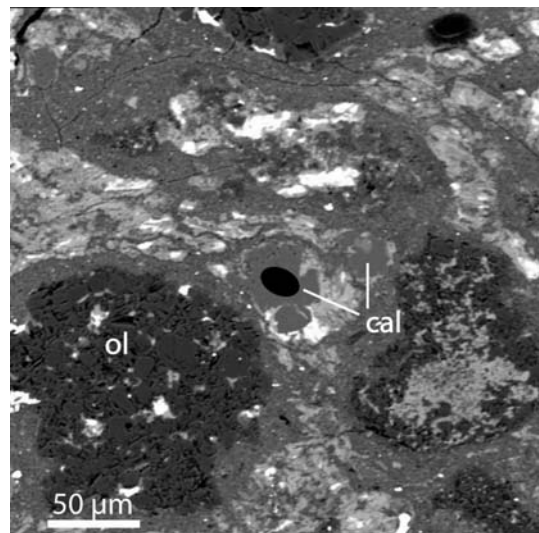
## Appendix 2

**Figure 16.** Spot locations of SIMS oxygen isotopic analyses. The methods employed are explained in the chapter 3 methods section. The term “bx#” indicates a specific area on a slide, so duplicates indicate the spots were in close proximity. Different letters indicate discrete grains. The photographs refer to data within Table 5, which shows the obtained results.

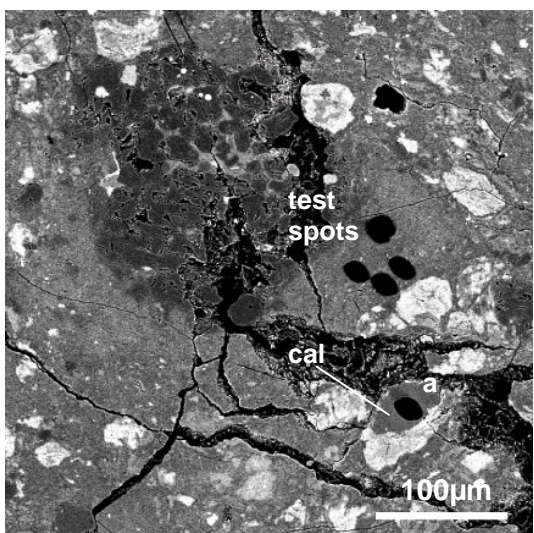
EET96006\_bx2



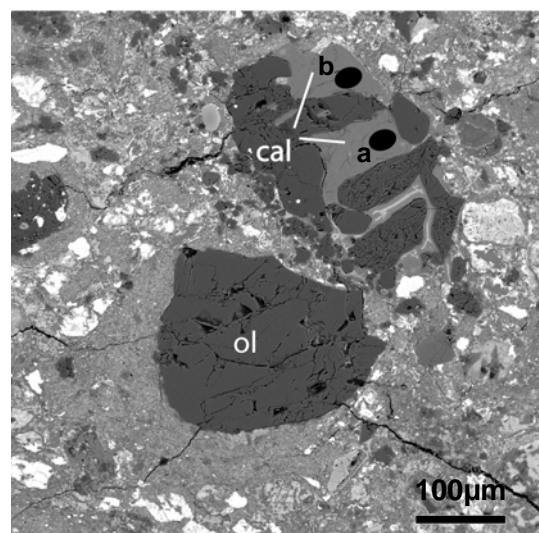
EET96006\_bx2



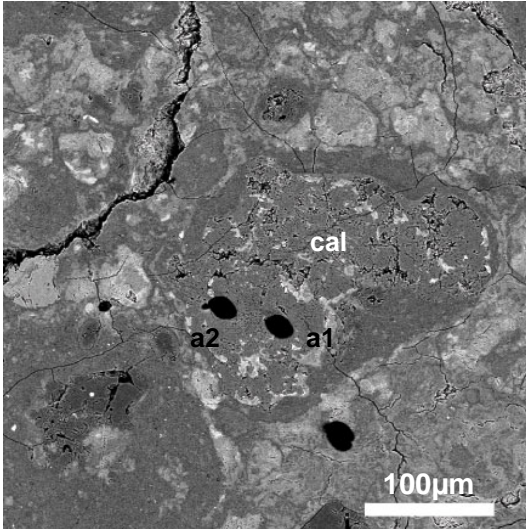
EET96006\_bx4



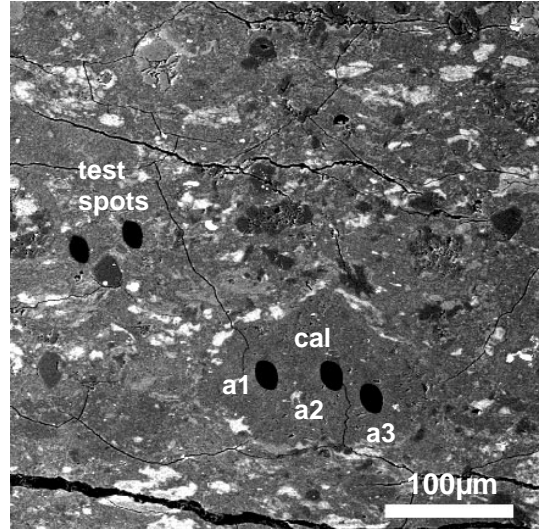
EET96006\_bx11



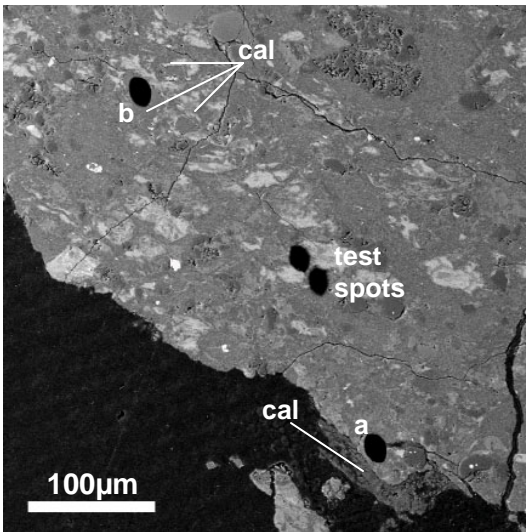
EET96006\_bx3



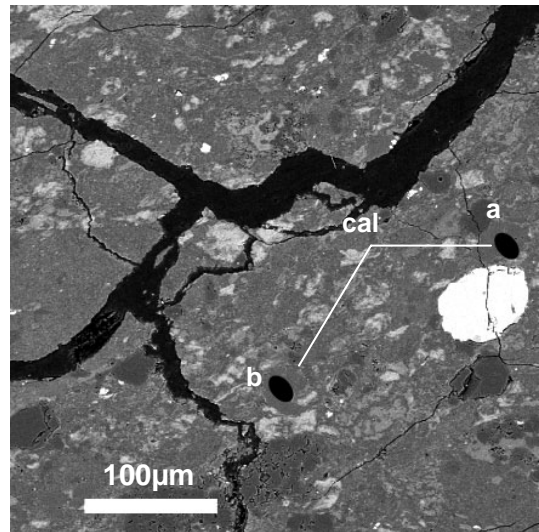
EET96016\_bx9



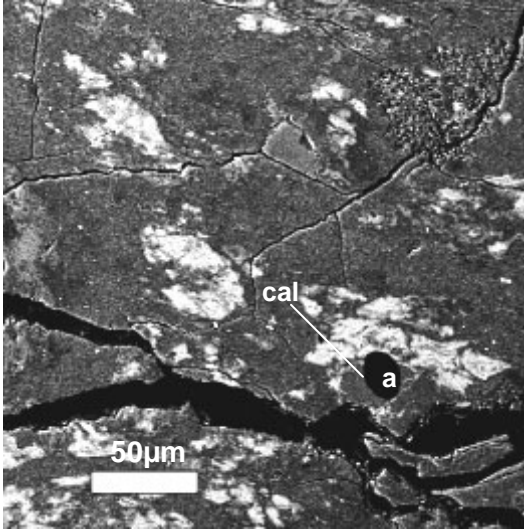
EET96016\_bx12



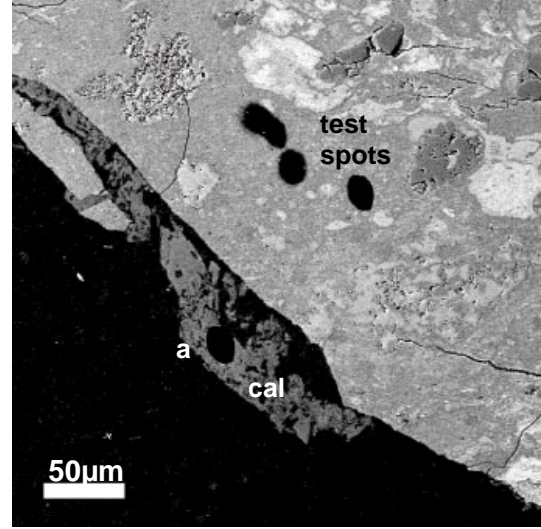
EET96016\_bx15



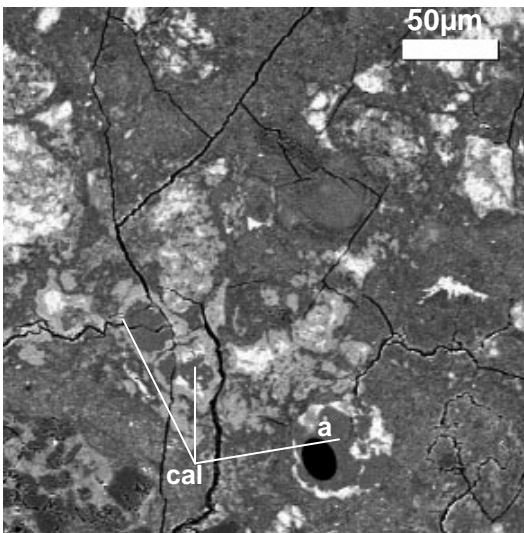
EET96016\_bx18



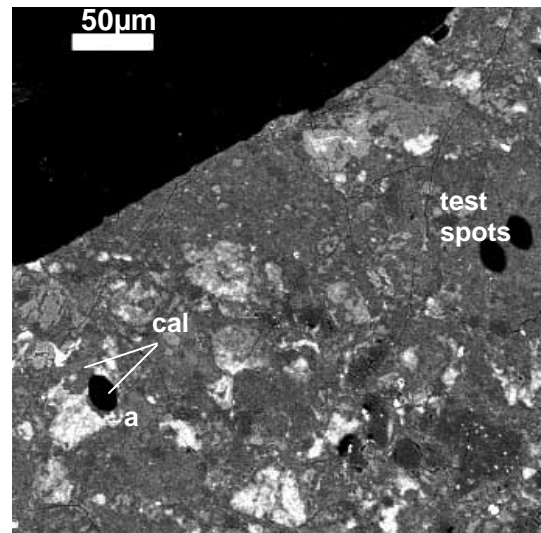
EET96016\_bx20



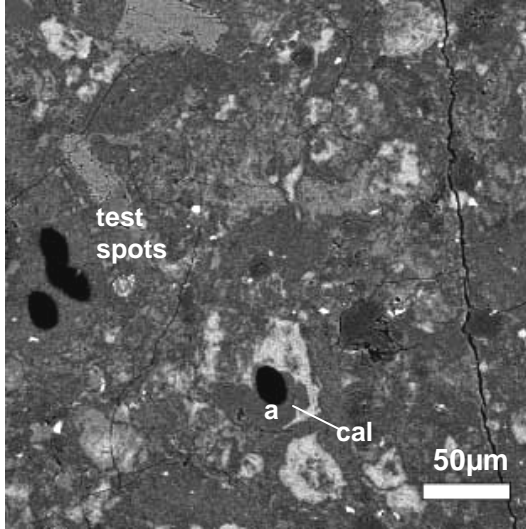
EET96017\_bx4



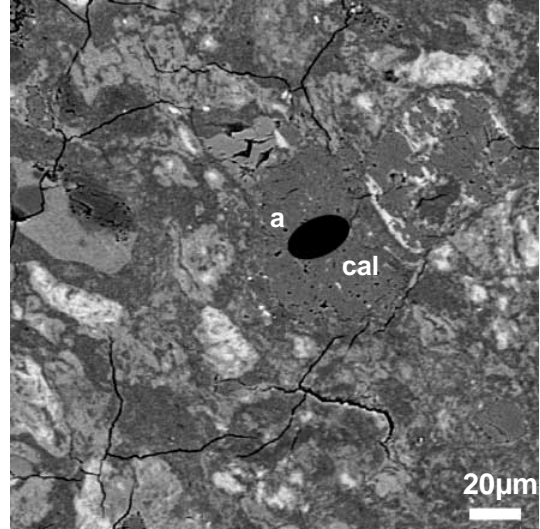
EET96017\_bx15



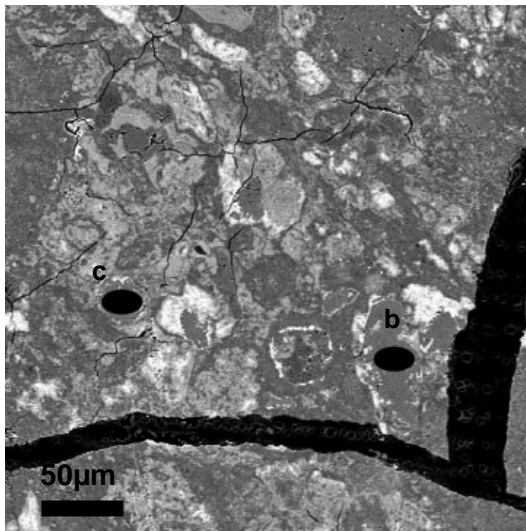
EET96017\_bx16



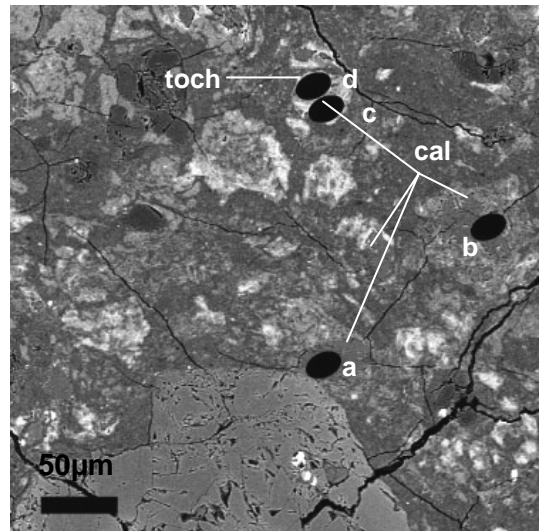
EET96019\_bx9



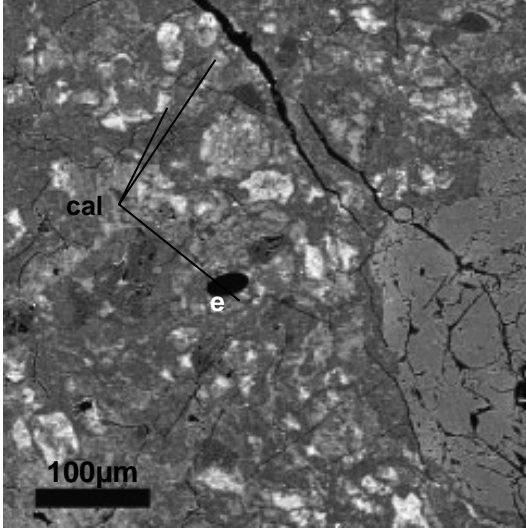
EET96019\_bx9



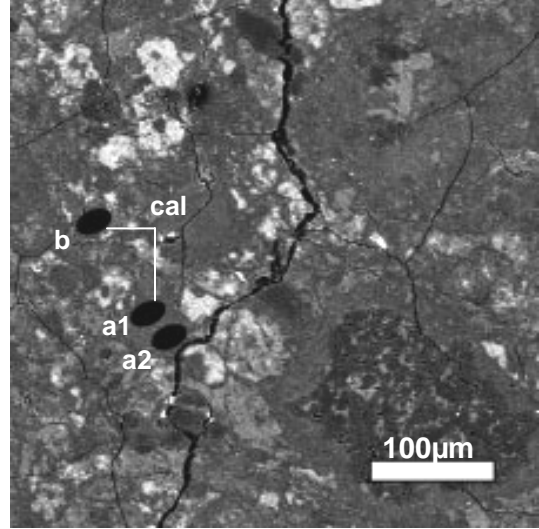
EET96019\_bx16



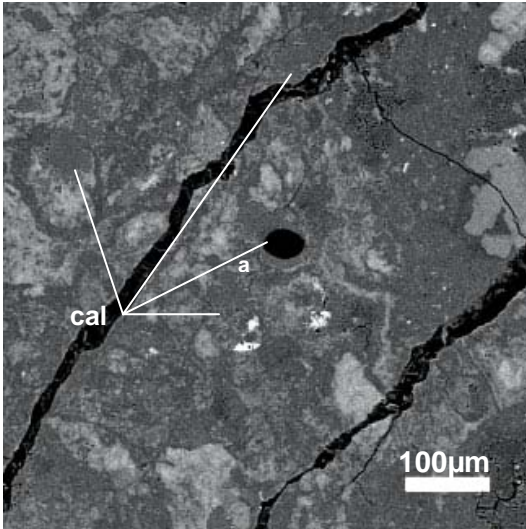
EET96019\_bx16



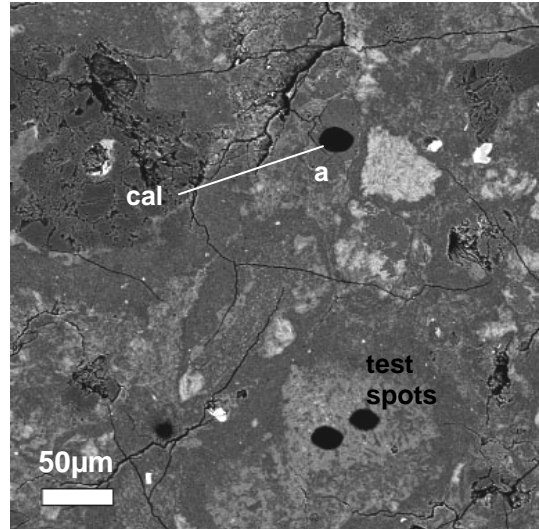
EET96019\_bx18



EET96019\_bx19



EET96019\_bx20



## Bibliography

- Airieau S. A., Farquhar J., Thiemens M. H., Leshin L. A., Bao H., and Young E. (2005) Planetesimal sulfate and aqueous alteration in CM and CI carbonaceous chondrites. *Geochimica et Cosmochimica Acta*, (in press).
- Barber D. J. (1981) Matrix phyllosilicates and associated minerals in CM2 carbonaceous chondrites. *Geochimica et Cosmochimica Acta* **45**, 945-970.
- Benedix G., Leshin L., Farquhar J., Jackson T., and Thiemens M. (2003) Carbonates in CM2 chondrites: Constraints on alteration conditions from oxygen isotopic compositions and petrographic observations. *Geochimica et Cosmochimica Acta* **67**(8), 1577-1588.
- Benoit P. H. (1995) Meteorites as surface exposure time markers on the blue ice fields of Antarctica--Episodic ice flow in Victoria-land over the last 300,000 years. *Quaternary Science Reviews* **14**(5), 531-540.
- Benoit P. H., Roth J., Sears H., and Sears D. W. G. (1994) The natural thermoluminescence of meteorites .7. Ordinary chondrites from the Elephant Moraine region, Antarctica. *Journal of Geophysical Research--Planets* **99**(E1), 2073-2085.
- Benoit P. H. and Sears D. W. G. (1992) Natural thermoluminescence of meteorites and implications for ice movement in the elephant moraine region. *Antarctic Journal of the United States* **27**(5), 28-31.
- Benoit P. H., Sears D. W. G., Akridge J. M. C., Bland P. A., Berry F. J., and Pillinger C. T. (2000) The non-trivial problem of meteorite pairing. *Meteoritics & Planetary Science* **35**(2), 393-417.
- Bland P., Bevan A., and Jull A. (2000) Ancient meteorite finds and the earth's surface environment. *Quaternary Research* **53**(2), 131-142.
- Bland P. A., Sexton A. S., Jull A. J. T., Bevan A. W. R., Berry F. J., Thornley D. M., Astin T. R., Britt D. T., and Pillinger C. T. (1998) Climate and rock weathering: A study of terrestrial age dated ordinary chondritic meteorites from hot desert regions. *Geochimica et Cosmochimica Acta* **62**(18), 3169-3184.
- Brearley A. J. and Jones R. H. (1998) Chondritic Meteorites. In *Planetary Materials*, Vol. 36 (ed. J. J. Papike), pp. 3.1-3.398. The Mineralogical Society of America.
- Brearley A. J., Saxton J. M., Lyon I. C., and Turner G. (1999a) Carbonates in the Murchison CM chondrite: CL characteristics and oxygen isotopic compositions. *Lunar and Planetary Science* **XXX**, 1301.pdf.
- Brearley A. J., Saxton J. M., Lyon I. C., and Turner G. (1999b) Carbonates in the Murchison CM chondrite: CL characteristics and oxygen isotopic compositions. *Lunar and Planetary Science abstract* **XXX**, 1301.pdf.
- Browning L., McSween H., and Zolensky M. (1996) Correlated alteration effects in CM carbonaceous chondrites. *Geochimica et Cosmochimica Acta* **60**(14), 2621-2633.
- Buddhue J. D. (1957) *The oxidation and weathering of meteorites*. University of New Mexico Press.

- Bunch T. E. and Change S. (1980) Carbonaceous chondrites .2. Carbonaceous chondrite phyllosilicates and light-element geochemistry as indicators of parent body processes and surface conditions. *Geochimica et Cosmochimica Acta* **44**(10), 1543-1577.
- Burbine T. H. (1998) Could G-class asteroids be the parent bodies of the CM chondrites? *Meteoritics & Planetary Science* **33**, 253-258.
- Cassidy W., Harvey R., Schutt J., Delisle G., and Yanai K. (1992) The meteorite collection sites of Antarctica. *Meteoritics* **27**(5), 490-525.
- Cassidy W., Meunier T., Buchwald V., and Thompson C. (1983) Search for meteorites in the Allan Hills/Elephant Moraine area. *Antarctic Journal of the United States* **18**(5), 81-82.
- Clayton R. and Mayeda T. (1999a) Oxygen isotope studies of carbonaceous chondrites. *Geochimica et Cosmochimica Acta* **63**(13-14), 2089-2104.
- Clayton R. N. and Mayeda T. K. (1984) The Oxygen Isotope Record in Murchison and other Carbonaceous Chondrites. *Earth and Planetary Science Letters* **67**(2), 151-161.
- Clayton R. N. and Mayeda T. K. (1999b) Links among CI and CM chondrites. *Lunar and Planetary Science XXX*, 1795.pdf.
- Consolmagno G. J., Britt D. T., and Stoll C. P. (1998) The porosities of ordinary chondrites: Models and interpretation. *Meteoritics & Planetary Science* **33**(6), 1221-1229.
- Donahue D. J. (1995) Radiocarbon analysis by accelerator mass spectrometry. *International Journal of Mass Spectrometry and Ion Processes* **143**, 235-245.
- Donahue D. J., Linick T. W., and Jull A. J. T. (1990) Isotope-ratio and background corrections for accelerator mass spectrometry radiocarbon measurements. *Radiocarbon* **32**(2), 135-142.
- Farquhar J. and Thiemens M. (2000) Oxygen cycle of the Martian atmosphere-regolith system:  $\Delta^{17}\text{O}$  of secondary phases in Nakhla and Lafayette. *Journal of Geophysical Research, planets* **105**(E5), 11991-11997.
- Farquhar J., Thiemens M., and Jackson T. (1998) Atmosphere-surface interactions on Mars: Delta O-17 measurements of carbonate from ALH 84001. *Science* **280**(5369), 1580-1582.
- Farver F. R. (1994) Oxygen self-diffusion in calcite: Dependence on temperature and water fugacity. *Earth and Planetary Science Letters* **121**, 575-587.
- Faure G. (1986) Cosmogenic Carbon-14 and Tritium. In *Principles of Isotope Geology* (ed. G. Faure), pp. 386-425. John Wiley and Sons.
- Faure G. (1990) Marine microfossils in till clasts of the Elephant Moraine on the east antarctic ice sheet. *Antarctic Journal of the United States* **25**, 23-25.
- Faure G., Hoefs J., Jones J., Curtis J. B., and Pride D. E. (1988) Extreme O-18 Depletion in Calcite and Chert Clasts from the Elephant Moraine on the East Antarctic Ice-sheet. *Nature* **332**(6162), 352-354.
- Faure G. and Taylor K. (1985) The geology and origin of the Elephant Moraine on the east antarctic ice sheet. *Antarctic Journal of the United States* **20**, 11-12.
- Faure G., Wehn K. S., Montello J. M., Hagen E. H., Strobel M. L., and Johnson K. S. (1993) Isotope composition of the ice and sub-glacial geology near the Allan

- Hills, Victoria Land, Antarctica. In *Gondwana Eight* (ed. Findlay, Unrug, Banks, and Veevers).
- Fredriksson K. and Kerridge J. F. (1988) Carbonates and sulfates in CI chondrites--formation by aqueous activity on the parent body. *Meteoritics* **23**(1), 35-44.
- Friedman I. and O'Neil J. (1977) Compilation of stable isotope fractionation factors of geochemical interest. *Prof. Pap. 440-KK. U.S. Geological Survey*.
- Fuchs L. H., Olsen E., and Jensen J. (1973) Mineralogy, Mineral-Chemistry, and Composition of the Murchison (C2) Meteorite. *Smithsonian Contributions to the earth sciences* **10**, 1-38.
- Goel P. S. and Kohman T. P. (1962) Cosmogenic carbon-14 in meteorites and terrestrial ages of "finds" and craters. *Science* **136**(3519), 875-876.
- Grady M. M., Wright I. P., Swart P. K., and Pillinger C. T. (1988) The carbon and oxygen isotopic composition of meteoritic carbonates. *Geochimica et Cosmochimica Acta* **52**(12), 2855-2866.
- Grossman J. N. and Score R. (1996) The Meteoritical Bulletin, No 79, 1996 July: Recently classified specimens in the United States Antarctic Meteorite Collection (1994-1996). *Meteoritics and Planetary Science* **31**, A0161-A174.
- Harvey R. (2003) The origin and significance of Antarctic meteorites. *Chemie der Erde-Geochemistry* **63**(2), 93-147.
- Huss G. R. (1990) Meteorite infall as a function of mass: Implications for the accumulation of meteorites on Antarctic ice. *Meteoritics* **25**(41-56).
- Johnson C. A. and Prinz M. (1993) Carbonate compositions in CM and CI chondrites, and implications for aqueous alteration. *Geochimica et Cosmochimica Acta* **57**(12), 2843-2852.
- Jull A. J. T., Cheng S., Gooding J. L., and Velbel M. A. (1988) Rapid growth of magnesium-carbonate weathering products in a stony meteorite from Antarctica. *Science* **242**(4877), 417-419.
- Jull A. J. T., Donahue D. J., and Linick T. W. (1989) Carbon-14 activities in recently fallen meteorites and Antarctic meteorites. *Geochimica et Cosmochimica Acta* **53**, 2095-2100.
- Jull A. J. T., Eastoe C. J., and Herzog G. F. (1995) Isotopic composition of carbonates in the SNC meteorites Allan Hills 84001 and Nakhla. *Meteoritics* **30**(311-318).
- Jull A. K. J., Courtney C., Jeffrey D. A., and Beck J. W. (1998) Isotopic evidence for a terrestrial source of organic compounds found in Martian meteorites Allan Hills 84001 and Elephant Moraine 79001. *Science* **279**, 366-369.
- Jull A. T., Eastoe C. J., and Cloudt S. (1997) Isotopic composition of carbonates in the SNC meteorites, Allan Hills 84001 and Zagami. *Journal of Geophysical Research*, **102**(E1), 1663-1669.
- Kerridge J. and Matthews M. (1988) *Meteorites and the Early Solar System*. The University of Arizona Press.
- Kopp R. E. and Humayun M. (2003) Kinetic model of carbonate dissolution in Martian meteorite ALH84001. *Geochimica et Cosmochimica Acta* **67**(17), 3247-3256.
- Labotka T. C., Cole D. R., and Riciputi L. R. (2000) Diffusion of C and O in calcite at 100 MPa. *American Mineralogist* **85**, 488-494.

- Lee M. R. and Bland P. A. (2004) Mechanisms of weathering of meteorites recovered from hot and cold deserts and the formation of phyllosilicates. *Geochimica et Cosmochimica Acta* **68**(4), 893-916.
- Lindstrom M., BcBride K., Mason B., and McCoy T. (1998) Curator's comments. *Antarctic Meteorite Newsletter* **21**(1), 17.
- Miller M. F. (2002) Isotopic fractionation and the quantification of O-17 anomalies in the oxygen three-isotope system: an appraisal and geochemical significance. *Geochimica et Cosmochimica Acta* **66**(11), 1881-1889.
- Nishiizumi K., Elmore D., and Kubik P. W. (1989) Update on terrestrial ages of Antarctic meteorites. *Earth and Planetary Science Letters* **93**(4-Mar), 299-313.
- Rasberry S. D. (1983) International standard reference material for contemporary carbon-14 oxalic acid SRM 4990C. National Bureau of Standards.
- Riciputi L. R., McSween H. Y., Jonson C. A., and Prinz M. (1994) Minor and trace-element concentrations in carbonates of carbonaceous chondrites, and implications for the compositions of co-existing fluids. *Geochimica et Cosmochimica Acta* **58**(4), 1343-1351.
- Rivkin A. S., Davies J. K., Johnson J. R., Ellison S. L., Trilling D. E., Brown R. H., and Lebofsky L. A. (2003) Hydrogen concentrations on C-class asteroids derived from remote sensing. *Meteoritics & Planetary Science* **38**(9), 1383-1398.
- Rowe M. W., Clayton R. N., and Mayeda T. K. (1994) Oxygen isotopes in separated components of CI and CM meteorites. *Geochimica et Cosmochimica Acta* **58**(23), 5341-5347.
- Ruddiman W. F. (2001) *Earth's Climate: Past and Future*. W.H. Freeman and Company.
- Schultz L. (1986) Allende in Antarctica: Temperatures in Antarctic meteorites. *Meteoritics* **21**(4), 505.
- Sharp Z. D. (1990) A laser-based microanalytical method for the in situ determination of oxygen isotope ratios of silicates and oxides. *Geochimica et Cosmochimica Acta* **54**, 1353-1357.
- Slota P. J. (1987) Preparation of small samples for <sup>14</sup>C accelerator targets by catalytic reduction of CO. *Radiocarbon* **29**, 303-306.
- Stuiver M. and Polach H. A. (1977) Discussion : Reporting of <sup>14</sup>C Data. *Radiocarbon* **19**(3), 355-363.
- Stuiver M. and Quay P. D. (1981) Atmospheric C-14 Changes resulting from fossil-fuel CO<sub>2</sub> release and cosmic-ray flux variability. *Earth and Planetary Science Letters* **53**, 349-362.
- Velbel M., Long D., and Gooding J. (1991) Terrestrial weathering of Antarctic stone meteorites: Formation of Mg-carbonates on ordinary chondrites. *Geochimica et Cosmochimica Acta* **55**, 67-76.
- Velbel M. A. (1988) The distribution and significance of evaporitic weathering products on Antarctic meteorites. *Meteoritics* **23**, 151-159.
- Young E., Ash R., England P., and Rumble D. (1999) Fluid flow in chondritic parent bodies: Deciphering the compositions of planetesimals. *SCIENCE* **286**(5443), 1331-1335.

- Zheng Y. F. (1999) Oxygen Isotope Fractionation in Carbonate and Sulfate Minerals. *Geochemical Journal* **33**, 109-126.
- Zolensky M., Mittlefehldt D., Lipschutz M., Wang M., Clayton R., Mayeda T., Grady M., Pillinger C., and Barber D. (1997) CM chondrites exhibit the complete petrologic range from type 2 to 1. *Geochimica et Cosmochimica Acta* **61**(23), 5099-5115.